Review

Merging solution processing and printing for sustainable fabrication of Cu(In,Ga)Se₂ photovoltaics

Bruna F. Gonçalves [a,b,c], Sascha Sadewasser [a], Laura M. Salonen [a], Senentxu Lanceros-Méndez [b,d,e], Yury V. Kolen'ko [a,*]

[a] International Iberian Nanotechnology Laboratory, Braga 4715-330, Portugal
[b] Center of Physics, University of Minho, Braga 4710-057, Portugal
[c] Center of Chemistry, University of Minho, Braga 4710-057, Portugal
[d] BCMaterials, Basque Center for Materials, Applications and Nanostructures, UPV/EHU Science Park, 48940 Leioa, Spain
[e] Ikerbasque, Basque Foundation for Science, 48009 Bilbao, Spain

ARTICLE INFO

ABSTRACT

The targeted global decarbonization demands the urgent replacement of conventional fossil fuel with low carbon technologies. For instance, solar energy is abundant, inexhaustible, non-polluting, and low-priced; however, to produce energy on a large scale with reliable, cost-efficient, and environmentally friendly methods remains a challenge. The outstanding optical properties of Cu(In,Ga)Se₂ thin film photovoltaics and their intrinsic compatibility with industrial-scale production are paving the way towards this technology. However, most of the activity in the field relies on the use of non-environmentally friendly methodologies to achieve solution-processed flexible and lightweight photovoltaics with significant efficiencies. Importantly, there is a search for more sustainable alternatives that are compatible with roll-to-roll industry to improve the cost-effectiveness and sustainability of photovoltaics without compromising the photovoltaic performance.

Herein, we review cost-efficient and sustainable fabrication methodologies that complement the current high-energy-demanding vacuum-based fabrication of Cu(In,Ga)Se₂ photovoltaics. The existent non-vacuum deposition methods of Cu(In,Ga)Se₂ photoabsorbers are presented and precursors and solvents used in ink formulations are discussed in terms of sustainability. The approaches resulting in most efficient photovoltaic cells are highlighted. Finally, all-solution-processed Cu(In,Ga)Se₂ photovoltaics are reviewed, along with the non-vacuum deposition methods of the individual layers, contributing to an even higher throughput and low-cost production. This review highlights the relevance and potential of sustainable non-vacuum methodologies, as well as the need of further investigation in this field to ultimately give access to high-end CIGS PVs with low-cost fabrication.

1. Introduction

Solar cells have emerged as the widespread photovoltaic (PV) technology for harvesting and delivering clean energy in numerous sectors across our society (Fig. 1). Owing to the abundant and inexhaustible nature of the solar energy, the broader application of solar cells would effectively support the reduction of greenhouse gas emissions [1] via transitioning from fossil-fuel-based power to renewable solar energy, thus greatly contributing to the realization of the Paris Agreement [2] and the European Green Deal [3].

In the past decades, PVs have been the subject of extensive research, and the continuous development of photoabsorber materials and PV engineering approaches has led to the realization of four generations of solar cells [4]. First-generation PVs are based on silicon, and they are the most mature and commercialized technology. Second-generation comprises direct band gap photoabsorbers with a few micrometers of thickness. Third-generation uses organic semiconductors relying on several energy levels and multiple charge carrier generation. Finally, the emerging fourth generation combines flexible polymeric thin films with nanoparticle (NP) structures to produce thin multi-spectrum layers (tandem PVs) [4,5].

With regard to the sustainability of the PVs, despite being a zero-net emission technology, the processes and methodologies used for the PV fabrication result, directly or indirectly, in the emission of CO₂. Interesting aspects in this regard, also associated to life-cycle assessment,

Nomenclature

AM1.5G	Global standard spectrum	NW	Nanowire
CIGS	Copper indium gallium diselenide	PV	Photovoltaic
E_C	Conduction band energy	QNR	Quasi-neutral region
E_F	Fermi energy	R_S	Sheet resistance
E_V	Valence band energy	RTA	Rapid thermal annealing
FTO	Fluorine-doped tin oxide	SCR	Space charge region
IPA	Isopropanol	SLG	Soda-lime glass
ITO	Tin-doped indium oxide	T	Temperature
J_{SC}	Short-circuit current	T_{550nm}	Transmittance at 550 nm
NP	Nanoparticle	TCO	Transparent conductive oxide
		ϕ_B	Barrier height

have been addressed by several authors [6,7]. Moreover, the end-of-life of the PVs also plays an important role in their sustainability since these materials might become hazardous waste if not recovered or disposed of properly. To guarantee the sustainability of the PV modules, it is very important to establish end-of-life management strategies [8] with low-cost recycling technologies. Europe, Japan, and United States are leading the research and development of PV module recycling, especially for silicon PVs.

Seminal reports of solar cells with Cu(In,Ga)Se$_2$ (CIGS) photoabsorber [9,10], extensive investigations of the material, PV cell design, and optimization studies have resulted in an interesting class of second-generation thin film PVs [11]. Already 1% (1284 MW) of the global solar energy is currently produced by CIGS PV technology [12]. CIGS is a semiconductor with a high absorption coefficient ($\approx 10^5$ cm^{-1}) and a direct band gap that can be tuned from 1.0 eV to 1.7 eV by changing the chemical composition. For instance, Cu(In$_{1-x}$Ga$_x$)Se$_2$ with $x = 0$ exhibits a band gap of 1.0 eV, while when $x = 1$, the band gap increases to 1.7 eV. The optoelectronic characteristics allow for the development of CIGS PVs with photoabsorber layer as thin as 1–2 μm, rendering the resultant thin film CIGS PVs an appealing alternative to the traditional first-generation silicon solar cells, which typically feature thicknesses of about 100 μm [13].

CIGS PVs are typically fabricated by a diversity of vacuum-deposition methods (*vide infra*) [14,15]. Notably, such methods are energy-demanding and expensive, and therefore there is a search for low-cost processing methods based on lower energy-demanding processes. The goal of this review is to illustrate the utility of sustainable non-vacuum methodologies that can offer low-cost fabrication of high-end CIGS PVs. We will focus on solution processing and printing deposition, as well as associated thermal treatments and inherent chemistry of solutions, specifically the nature of the solvent and the precursors.

2. CIGS PVs

CIGS PVs can have substrate or superstrate cell configurations. In the first case, light passes through a transparent front contact layer, whereas in the superstrate configuration light passes through a transparent substrate and reaches the active layer. Substrate configuration is the most common one, since it provides the most efficient PV cells due to favorable processing conditions [16].

Theoretically, for a non-concentrated system under AM1.5G illumination, the Shockley−Queisser limit determines that the maximum solar conversion efficiency for a single *p–n* junction CIGS PV cell is ≈33.7%, which happens at a band gap of 1.34 eV [17]. This theoretical limit
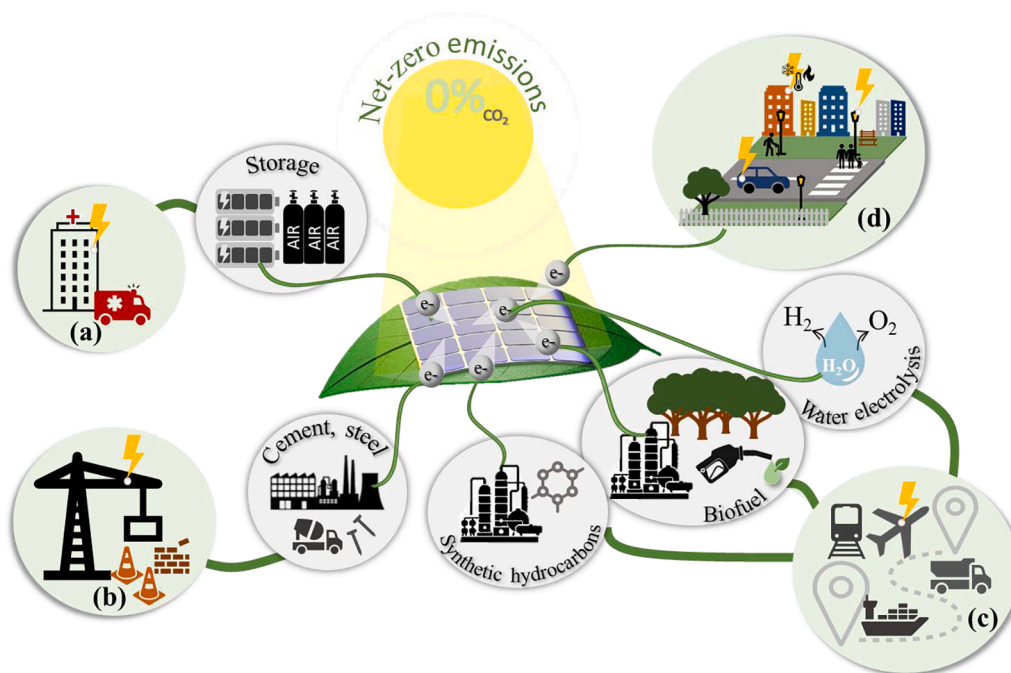

Fig. 1. Solar energy powered services: (a) highly reliable electricity in buildings, (b) structural materials production, (c) aviation, long-distance transportation/shipping, and (d) small transportation, light, heating/cooling.

considers (*i*) non-absorbed photons below the photoabsorber band gap, (*ii*) thermalized energy of photons above the photoabsorber band gap, (*iii*) voltage loss from thermal radiation, and (*iv*) absence of ohmic losses of the PV cells [18]. At the same time, the champion CIGS PVs have experimentally reached efficiencies of 23.35% [19] and 18.6% [20] on the cell and module levels, respectively.

The common structure of a CIGS PV (a, b), together with the respective band alignment (c) are depicted in Fig. 2. The PV device has a complex layered structure consisting of soda-lime glass (SLG)/Mo/ CIGS/CdS/*i*–ZnO/ZnO:Al, wherein (*i*) SLG is the PV substrate; (*ii*) Mo is the back contact coated on SLG; (*iii*) CIGS is the *p*-type photoabsorber thin film of copper indium gallium diselenide; (*iv*) CdS is the buffer layer of *n*-type cadmium sulfide; (*v*) *i*-ZnO is the resistive layer of intrinsic zinc oxide; and finally (*vi*) ZnO:Al is a transparent conducting window layer of aluminum-doped zinc oxide.

As substrate, rigid SLG is very commonly used in CIGS PVs (Fig. 2a, b), mostly due to its high thermal stability and capability of supplying sodium to the CIGS layer during fabrication, which increases the PV cell efficiency. Equally interesting stainless-steel foil [22] and polyimide [23] are employed as well, which provide lightweight flexible PV cells with reduced cost and easy reorientation to sunlight. Importantly, such flexible substrates are also suitable for roll-to-roll large-scale fabrication processes.

With regard to current collection, the most commonly used back contact is Mo (Fig. 2a, b). This is mainly due to its high electrical conductivity (5×10^{-6} Ω cm) and good corrosion resistance. Additionally, Mo forms a very thin layer of $MoSe_2$ at the interface with the CIGS photoabsorber (Fig. 2b), thus providing a quasi-ohmic contact between the Mo back contact and the photoabsorber [24]. Transparent conductive oxide (TCO) substrates, e.g., tin-doped indium oxide (ITO) [25] and fluorine-doped tin oxide (FTO) [26], have also been successfully employed in CIGS PV cells. In addition to being useful for applications that require transparency [27], when combined with metallic reflectors, the reflectivity of TCOs can be enhanced as compared to Mo-coated SLG [28].

The stoichiometry [Cu] / [In + Ga] = 0.9 and [Ga] / [In + Ga] = 0.3 is essential to obtain highly efficient CIGS PV cells [29]. The presence of a Ga gradient in the photoabsorber thin film is very commonly observed, as it works as a passivation layer for the Mo back contact, protecting it from recombination of charge carriers. Notably, the recently explored ultrathin CIGS photoabsorbers (<1 µm) exhibit lower absorption of photons and higher recombination at the back contact. In this particular case, the Ga gradient is not sufficient to prevent charge recombination, and therefore passivation layers, such as Al_2O_3 [30], MgF_2 [31], SiO_2 [32], and TiO_2 [33], have been developed to be placed between the Mo back contact and the CIGS photoabsorber. Importantly, ultrathin CIGS photoabsorber layers significantly reduce the use of rare and expensive In and Ga elements and consequently the PV production costs, rendering them feasible for industrial scale production. PV cells with over 10% of efficiency have already been developed using only 450 nm thick CIGS thin films [34].

To create a *p–n* junction in high-efficiency CIGS PVs, CdS, with a band gap of 2.4 eV, is the most commonly used buffer layer (Fig. 2a, b) [24]. Alternatives, such as In_2S_3 [35], ZnTiO [36], $Zn_{1-x}Mg_xO$ [37], and Zn(O,S) [38], have also been successfully employed. The latter materials have larger band gaps than CdS, thus reducing optical losses inside the buffer layer, but more importantly, they circumvent the use of the toxic Cd metal [39].

TCOs are commonly used as front contacts owing to their high optical transparency (>85%) and low electrical resistivity ($\leq 10^{-3}$ Ω cm). High-performing CIGS PV cells employ bi-layered TCO consisting of a thin film of *i*-ZnO and a thicker film of ZnO:Al (Fig. 2a,b) [24]. Alternatively to the *i*-ZnO/ZnO:Al assembly, materials with large band gaps, such as ITO [40], $ZnO_{1-x}S_x$:Al [41], $Zn_{1-x}Mg_xO$:Al [42], ZnO:B, In_2O_3: Mo [43], and In_2O_3:H [44], have been employed as front contacts, thus increasing the transmission of ultraviolet photons to the CIGS photoabsorber.

The different band gap energies and electron affinities of the individual layers affect the band alignment and shape the discontinuity of the conduction band at the interfaces, producing a band diagram
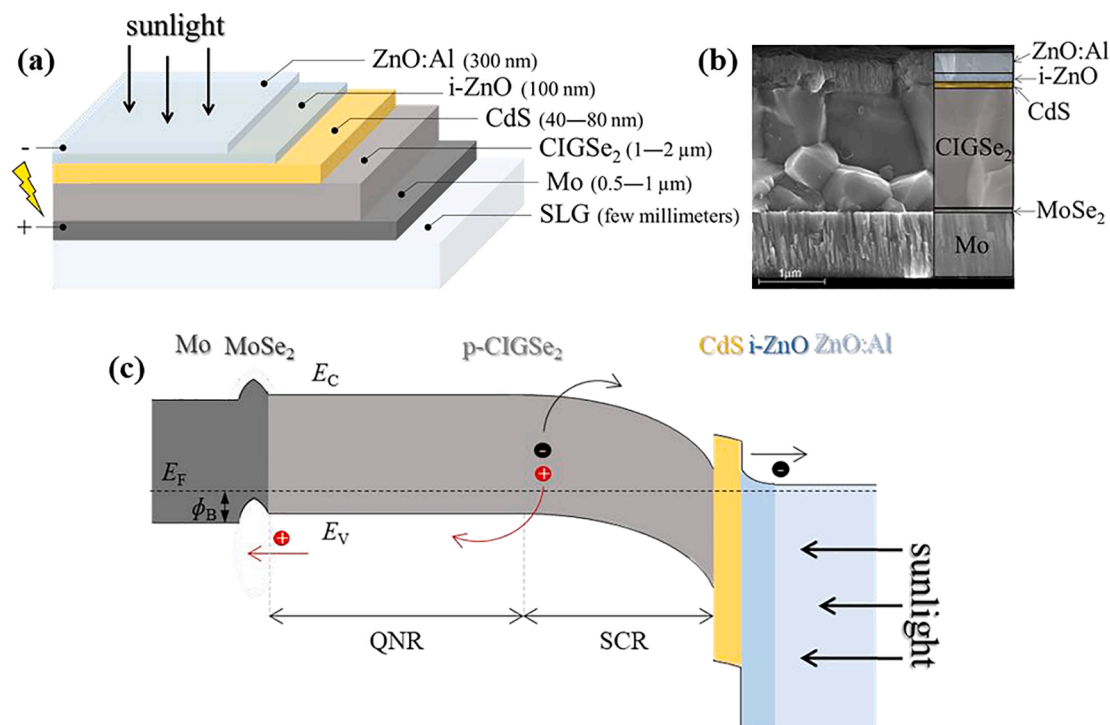

Fig. 2. Common layered structure of a CIGS PV device (a), together with the respective cross-section SEM image adapted from [21] (b) and a band diagram under equilibrium (c). E_C = conduction band energy, E_V = valence band energy, E_F = Fermi energy, SCR = space charge region, QNR = quasi-neutral region, ϕ_B = barrier height.

(Fig. 2c). At the interface between CIGS and CdS, a positive discontinuity of the conduction band, a spike, occurs. When the spike is too high, the flow of the charges from CIGS to the CdS layer is inhibited, reducing the short-circuit current (J_{SC}). When the spike is small, the electrons are thermally emitted across the spike, and the spike does not work as a barrier [45].

Advantageously, CIGS PV modules are very reliable, showing degradation of only ≈0.5% per year. The observed degradation can be attributed to (*i*) metastabilities, (*ii*) partial shading and hotspots, (*iii*) potential-induced degradation, and (*iv*) back contact issues [46]. Of the environmental factors, humidity has been established as the cause of the highest degradation rate of CIGS PVs, and encapsulation of the PV modules is performed to overcome this issue [47].

From the fabrication point of view, the most efficient CIGS PV cells are developed using vacuum-based deposition processes, which allow a fine control of the deposition parameters, thus affording reproducible fabrication of high-quality thin films (i.e., crystalline, phase pure, semiconducting, compact, smooth, etc.) [14]. For example, the most extensively developed large-area deposition techniques (sputtering, co-evaporation, physical or chemical vapor depositions) are industrially relevant vacuum-based methods for the fabrication of CIGS solar cell modules. On the other hand, small-area deposition methods (pulsed laser deposition, molecular beam epitaxy) are commonly used in the laboratory research to advance CIGS PVs.

In the typical scenario of CIGS PV fabrication, the Mo back contact is first deposited on a rigid or flexible substrate followed by the deposition of either alloy Cu–In–Ga or chalcogenide Cu–In–Ga–Se thin film. Next, the resultant film is subjected to so-called selenization – a gas-transport reaction in Se or H_2Se vapors for CIGS crystal growth under 450–600 °C – in order to obtain a high-quality CIGS photoabsorber layer. The PV device is then completed by the deposition of the aforementioned consecutive layers (Fig. 2), thus affording a high-performing CIGS solar cell.

The environmental impact of the devices during the whole life cycle is also relevant and, in particular, at the end of their functional life. To date, CIGS PV technology has just a few implemented recycling strategies. The processes of both NPC Inc. and Hamada Corporation are based on pyrolysis of polymers and grating of the chalcopyrite layer after removal of the frame and the backsheet. Loser Chemie has patented a process in which the semiconductor materials are recovered by a chemical treatment after crushing and separating the materials [48]. Large-scale chalcopyrite PV systems are currently recycled using a combination of mechanical and chemical treatments [49]. On the whole, in view of circular economy, recycling strategies are essential, and more are expected to emerge as the CIGS PVs move closer to commercialization.

3. The challenge

The major challenge in the commercialization and market uptake of second-generation CIGS PV technology is the high cost and the associated environmental impact of the PV fabrication [50]. For example, the champion CIGS PV with the complex cell structure SLG/Mo/CIG(S,Se)$_2$/CsF/Zn(O,S,OH)$_x$/ZnMgO/ZnO:B/Al/MgF$_2$ has been fabricated employing vacuum techniques [19], thus marking the high versatility and broad applicability of these methods. However, vacuum-based depositions are energy demanding, time consuming, and require expensive equipment. In addition, uniform film deposition over large substrate areas, essential for the production of working PV modules, poses a further challenge.

Printing and coating techniques provide new opportunities to develop sustainable strategies toward the fabrication of efficient CIGS PVs. The number of non-vacuum approaches has gradually increased in the recent years, since such methodologies not only enable challenging fabrication of CIGS PVs to be carried out in cost-efficient fashion with lower environmental impact, but also potentially afford large-scale fabrication via industrial roll-to-roll and screen printing processes.

4. Sustainable fabrication of CIGS PVs

Sustainable fabrication should: *i*) minimize waste and the input of non-renewable energy, *ii*) seek environmentally friendly source materials and products, and *iii*) plan for technology recycling from the beginning [51]. During the production of CIGS PVs, the layer deposition is the most energy-demanding step. Therefore, the replacement of vacuum-based deposition techniques with less energy demanding non-vacuum ones can have a large impact on the sustainability of the process. In addition, typically these processes are also associated with low amounts of material waste, or even none, when operating.

In printed/solution-processed PVs, both solvents and precursors used in ink formulations and/or chemical reactions are the components most contributing to the sustainability of the process. Importantly, green solvents and chemicals do not pose risks to the human health, safety, and the environment during their entire life cycle [52]. For the quantitative evaluation of the health, safety, and environmental impact of solvents, the "Global Harmonized System of Classification and Labeling of Chemicals" (GHS) established a list [53]. Based on the GHS, GlaxoSmithKline (GSK) keeps a regularly updated list that provides several sub-categories and rates the sustainability of the solvents using a parameter called composite score value (G), with a range of 1 to 10 from non-sustainable to sustainable [54]. Therefore, solvents with a high G score are appropriate for sustainable chemical procedures [55]. In addition to the source materials, by-products formed during processing should also be taken into consideration: for example, the thermal treatments employed for curing and sintering can release chemical vapors that are poisonous to humans and the environment. In such cases, thermal treatments should be avoided and replaced by sustainable alternatives. Finally, the recycling strategies of PV materials should be considered from the beginning and throughout all the production steps [56].

5. Printed/solution-processed CIGS PVs

Non-vacuum processes can be divided into three classes: (*i*) electrodeposition, (*ii*) particulate-based ink, and (*iii*) solution-based ink [57]. Electrodeposition is beyond the scope of this review and for an overview of this process, the readers are referred to the literature [58,59]. Particulate inks are suspensions of synthesized or commercial particles in solvents (Fig. 3a, b), whereas solution inks typically consist of metal salt precursors dissolved in a solvent (Fig. 3c). The formulated inks are further deposited on a substrate (Fig. 3d) and subjected to a thermal treatment when required (e.g., calcination, annealing, selenization) to produce a dense CIGS layer (Fig. 3e). Both particulate and solution approaches are perfectly fit for printing deposition of the thin film, but the rheological properties of the inks need to be tuned for the chosen printing method. At the moment, CIGS PVs with similar efficiencies of 17.1% and 17.3% have been achieved using printing technologies employing particulate [60] and solution-based [61] inks, respectively.

5.1. Nature of the ink precursors

With respect to particulate-based ink processing, the particles used can be either synthesized colloidal CIGS NPs or synthesized non-colloidal CIGS NPs as well as commercially available precursors, for instance, metal oxides. CIGS NPs have been synthesized by solvothermal [62], hydrothermal [63], hot-injection [64], heating-up [65,66], and mechanochemical [67] methods. Accordingly, Cu, In, Ga, and Se metals are used as elemental species or salts dissolved in organic solvents to react and produce a precipitate. Usually, these procedures provide nanocrystalline CIGS with precise phase and shape control. On the other hand, the scale-up of these procedures is hindered by the use of complex
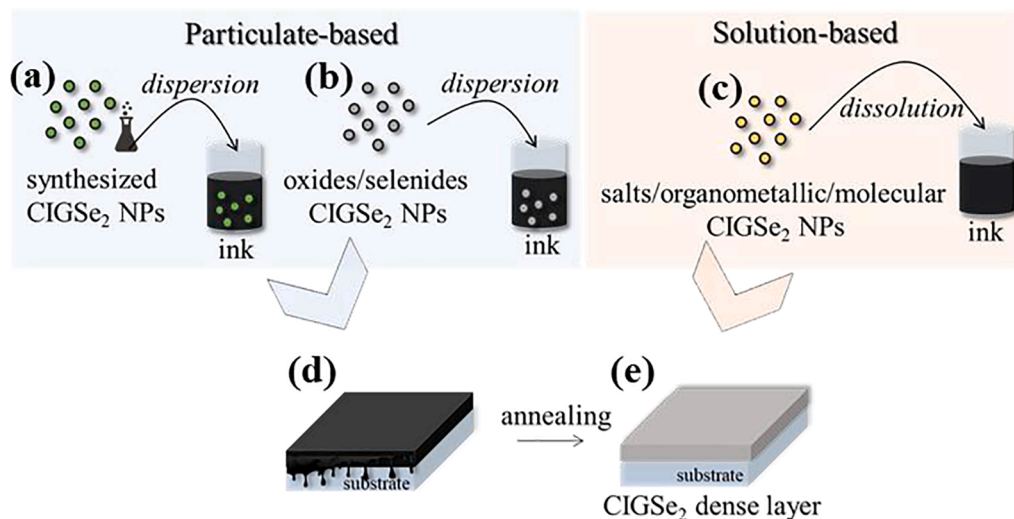
Fig. 3. Formation of inks for the CIGS layer using (a) particulate-based synthetic route, (b) particulate-based commercial route, and (c) solution-based process. (d) CIGS deposited film and (e) CIGS dense layer after annealing.

reaction set-ups incorporating autoclaves, Schlenk lines, or gloveboxes. Furthermore, these methods employ toxic organic solvents, such as hydrazine [68], ethylenediamine [62], and trioctylphosphine [69], as well as high boiling point solvents, such as oleylamine [70] and hexadecylamine [65,66] with reaction temperatures above 280 °C, resulting in carbon residues in the obtained films [71]. The highest PV cell efficiency obtained with a colloidal CIGS NP procedure is 15.0%, using hybrid solvothermal/hot-injection method with sulfur/oleylamine and subsequent selenization treatment to grow the crystal [72].

Environmentally friendly synthesis of colloidal or non-colloidal CIGS remains rather unexplored in the literature. Le and co-workers established a colloidal synthesis method with a simple experimental set-up based on sonochemistry with ethanol as solvent [73], while Juhaiman et al. reported a microwave-assisted colloidal synthesis using water and mercapto-acetic acid as solvents [74]. Chaure and co-workers, on the other hand, synthesized colloidal CIGS NPs and built a PV cell. Accordingly, a chemical ion reduction method was developed using polyethylene glycol as solvent and stabilizer and sodium borohydride as reducing agent, delivering a PV cell with 9.33% efficiency, the highest reported efficiency using environmentally-friendly synthesis of CIGS NPs [75]. Recently, reports have started to emerge on aqueous syntheses. We developed one delivering ~5 g of phase-pure non-colloidal CIGS NPs with tetragonal chalcopyrite structure and heterogeneous size distribution [76]. In another study, by using capping ligands (stabilizers), such as mercaptoacetic acid, glutathione, and citric acid tri-sodium, typical for non-aqueous synthesis of stable and uniform CIGS NPs, aqueous colloidal synthesis of quaternary chalcogenide Cu_2ZnSnS_4 NPs [77] and ternary $CuInSe_2$ NPs [78] have been realized. With these recent promising examples, we expect an increase in successful reports on aqueous colloidal synthesis of CIGS NPs in the future.

The commercial route, usually using metal oxides or selenides as precursors, uses a two-step thermal treatment to provide a dense and uniform CIGS layer, avoiding the need for stabilizers typically required in synthetic procedures. First, a thermal treatment (≈500 °C) with a reductive atmosphere converts the oxides to Cu–In–Ga alloy. Then, a selenization step (≈550 °C) is carried out to introduce Se and grow the crystal. The disadvantage of this method is the commonly observed Ga segregation on the back contact, which negatively impacts the PV performance. When using a mixture of solution/particulate-based processes with sequential chemical reactions starting with metals chips dissolved in acid to obtain metal oxides and followed by selenization, a maximum efficiency of 13.6% has been achieved for the PV cell [79]. In a process developed by the company Nanosolar, metal selenides were used as

precursors and subjected to a single thermal treatment and the resulting PV cell exhibited an efficiency of 17.1%, although Ga segregation was also identified as a problem [60].

The solution-based ink process employs metal salts (e.g. $Cu(NO_3)_2$), organometallic (e.g. $(PPh_3)_2CuIn(SEt)_4$) or molecular (e.g. Cu_2S in hydrazine) precursors in solution, thus omitting the need for stabilizers and leading to a homogenous layer composition with a lower number of defects than particulate-based inks. This process sometimes includes a final annealing treatment [29]. Of the different precursors used for the solution-based ink, the molecular approach has been shown to provide the highest efficiency PV cells (17.3%) [61]. This example, however, was achieved employing the highly toxic and explosive hydrazine, the use of which is not allowed at industrial-scale production. Green solutions using ethanol and propylene glycol followed by selenization treatment have delivered efficiencies of 8.0% and 12.4%, respectively [80,81].

Notably, the solution-based ink procedure delivers high-quality dense CIGS layers with uniform composition and thickness, avoiding the need of using additional chemicals to ensure the stability of the particles, which translates into a beneficial zero carbon content in the CIGS layer. This procedure is also the one delivering the maximum PV efficiency of the above-mentioned precursor approaches. The trade-off is the need of using non-environmentally friendly solvents, dangerous explosive chemical procedures (e.g. hydrazine), and/or selenization, which all can harm humans and the environment and are not compatible with roll-to-roll production.

Interestingly, the particulate-based ink procedure, especially when using commercial oxides, is a facile and inexpensive option and nanosized metal precursors can be easily sourced commercially. In addition, the oxide dispersion can be achieved using green solvents and environmentally benign additives, such as surfactants. However, a disadvantage of the process is the required selenization treatment to incorporate Se and grow the crystal. The selenization step can be avoided by using synthesized quaternary CIGS nanocrystals. However, most of the existent procedures employ toxic solvents and complex setups for their preparation, which renders their industrial implementation very complicated. Therefore, finding new, environmentally friendly, non-complex procedures for their synthesis that allow for upscaling for eventual uptake by the industry is of high importance and an area at which research efforts should be directed.

5.2. Selenization

Selenization is a crucial step in the formation of CIGS from metal oxide or nitrate precursors. It is a gas-transport reaction that occurs when a film containing Cu, In, and Ga precursors is exposed to a thermal treatment with Se vapor under controlled atmosphere. Se can be also supplied in the gas phase in the form of H_2Se, which speeds up the process and provides a more homogenous and larger crystals than those obtained by the use of elemental Se vapor. The lower toxicity of the latter renders it the more advantageous option. Independently of the Se source, this treatment can be used on both vacuum and non-vacuum deposited photoabsorber layers to grow the final CIGS crystal. In addition to the crystal growth, when using Mo back contacts, a thin layer of $MoSe_2$ is generated between the back contact and the photoabsorber layer producing a quasi-ohmic contact, which is beneficial for the PV cell efficiency [13].

The growth of the CIGS crystal is a complex process, rendering the control of the crystallization parameters challenging. After the initial growth of binary selenides of Cu and In, the $CuInSe_2$ phase grows at around 370–380 °C, followed by the $CuGaSe_2$ phase at around 425 °C. The complete growth of the $Cu(In,Ga)Se_2$ crystal occurs at $T > 500$ °C by the slow interdiffusion between $CuInSe_2$ and $CuGaSe_2$ along with Ga segregation towards the back contact. This segregation occurs due to the more favorable reaction between In and Se than Ga and Se and tends to create a lower energy band gap at the space charge region of the photoabsorber, leading to poor open-circuit voltage [82]. This can be overcome by performing sulfurization after selenization. Sulfurization is commonly used to improve the PV efficiency and can be carried out using three different methods: annealing the photoabsorber in H_2S atmosphere [83], evaporating In_2S_3 onto the photoabsorber and annealing in sulfur vapor [84], or by using elemental evaporation of sulfur [85], all non-compatible with industrial production.

Selenization can be carried out using rapid thermal annealing (RTA) or a one-step, two-step, or even three-step selenization procedure. RTA is a short and scalable thermal treatment [86], while two and three-step selenizations promote slow interdiffusion between $CuInSe_2$ and $CuGaSe_2$, ensuring their homogenization and therefore minimizing the Ga segregation towards the back contact [82]. All thermal treatments are carried out using a specific setup typically comprising a furnace and a horizontal quartz reactor tube to withstand high temperatures. The conditions of the process depend on the composition and deposition of the film and need to be optimized in terms of temperature, time, pressure, atmosphere, and Se concentration. In some cases, the films are placed inside a graphite box to ensure constant partial pressure and temperature to grow the CIGS crystals [87].

Despite being a very useful and effective procedure to gain access to large and homogenous crystals, selenization releases toxic vapors, which are hazardous to humans in large-scale production, rendering it non-suitable for roll-to-roll processes. In this respect, thin film deposition using ink formulations of CIGS NPs is advantageous by omitting the need of selenization. Nevertheless, obtaining a dense, compact, and carbon-free CIGS layer through this approach without high-temperature annealing, which prevents the use of polymeric substrates, remains a challenge. A possible solution could be femtosecond laser annealing, which does not require high temperatures and is compatible with industrial production. Such treatment has been demonstrated to enhance the efficiency of PV devices by decreasing both the shunt leakage current and recombination centers [88], thus providing a great approach to replace conventional annealing treatments.

5.3. Inks and deposition processes

The quality of the films is determined not only by the ink formulation, but also by the type of substrate and applied post-deposition treatments which also play a major role in both the cost and the range of applicability of the resulting PV cell. An ink formulation comprises a precursor, a solvent, and additives. In addition to the precursor quality, as discussed in the previous section, the solvent is the key element for a good dispersion/dissolution. Solvent polarity, reactivity, surface tension, viscosity, and volatility must be considered not only to adjust the properties of the ink for the chosen printing technique but also to guarantee suitable dispersion/dissolution of the precursors [89]. The use of additives, such as binders and surfactants, helps to adjust the viscosity and surface tension of the ink, improving its wettability, dispersion, and stability, thus resulting in dense and smooth CIGS layers, without grain boundaries. Binders are synthetic or natural polymers (e. g. polyvinyl alcohol and cellulose), and surfactants are ionic or non-ionic surface tension modifiers (e.g. sodium dodecyl sulfate and Triton X-100) [90]. The additives also enhance the integrity of the films by improving their adhesion to the substrate and preventing cracking and delamination during post-deposition thermal processes, detrimental to the performance of the device.

After ensuring appropriate ink viscosity for the selected deposition process, to achieve a smooth printed layer, the surface tension of the ink should be close to or lower than the surface energy of the substrate. To address the challenging high surface tension of aqueous systems, a combination of water with low-surface-tension solvents (e.g., ethanol) can be employed. Alternatively, the addition of hydrophilic chemical additives, such as cellulose-derived chemicals or polyvinyl alcohol, can assist in providing a well-printed film.

Particulate-based inks with synthetic precursors allow for a high control of the layer composition, and the only lack of homogeneity arises from the layer thickness, which does not affect the crystal stoichiometry. These NPs, when synthesized without stabilizers, need surfactants to produce an ink formulation with uniform composition. Although surfactants can provide a solution, they may leave residues even after annealing the films that compromise their quality, rendering the process challenging [90]. With commercial precursors, NP agglomeration is very common and leads to different settling rates in the solution, compromising the correct stoichiometry within the films. In such cases, the addition of a surfactant may lead to a uniform dispersion of the NPs, however, it may also leave carbon residues in the final film.

Inks from solution-based precursors are generally quite homogeneous on the molecular level and are often considered an excellent choice to achieve smooth layers with uniform composition. In this approach, the dissolution of the precursor is crucial, as incomplete dissolution can result in cracks and shrinkage of the films during annealing. Therefore, the ink components as well as the temperature and pH should be carefully tuned to allow for complete solubilization of the precursors and avoid premature precipitation [90].

The use of solution-based inks is a very effective approach to obtain uniform layers. However, the ink formulation requires specific chemical conditions (e.g., reaction temperature) and extra caution (e.g., controlled pH) to avoid morphological defects in the final CIGS layer, rendering it a complex procedure for industrial implementation. On the other hand, simple procedures can be employed for the ink formulation from particulate-based commercial precursors, but the mandatory use of selenization in the case of oxides to convert them into CIGS with uniform composition is very challenging and non-compatible with roll-to-roll fabrication. Finally, the use of particulate-based ink with synthetic procedure, preferably under aqueous conditions, is straightforward from the as-synthesized nanocrystals to the printed CIGS film. Nevertheless, the removal of stabilizers used during synthesis can cause defects in the printed layer, which work as recombination centers for charge carriers and therefore hamper the device performance. When stabilizers are impossible to avoid, the addition of a low content of stabilizers during synthesis that can be rapidly degraded, preferably environmentally benign ones (e.g., glutathione), as well as employing nanocrystals with homogeneous size distribution will allow to obtain uniform and defect-free CIGS printed layers without grain boundaries.

The most relevant deposition techniques to produce CIGS films are spin coating, blade coating, inkjet printing, spray coating, and screen

printing (Fig. 4), and their main advantages, limitations, and principal parameters are presented in Table 1. To evaluate several factors related to the sustainability of these fabrication methods, such as solvents/additives and the nature of precursors used in ink formulation, deposition processes, and thermal treatments employed, a color code is introduced, where red and green colors stand for high and low environmental/ health impacts, respectively.

From these techniques, spin coating provides the most efficient CIGS PV cells, with the highest efficiency reported of 17.3% [61]. Additionally, the advantages include simplicity, low cost, and omitting the need for rheology additives. However, a significant amount of material is wasted during the ink deposition, and the resultant layers have nanometric size thicknesses, leading to repeated depositions until obtaining micrometer size thick films. Finally, and more importantly, the noncompatibility of spin coating with roll-to-roll industry limits its employment in the scale-up production of PVs.

Blade coating, in addition to compatibility with roll-to-roll industry, is very simple, cost-efficient, and the second most efficient deposition process. CIGS PV cells prepared using this technique have reached efficiency of up to 15.0% [72]. On the other hand, spray coating allows for higher throughput than blade coating, and spray-coated CIGS PV cells have reached maximum efficiency of 10.7% [91]. However, both methods suffer from low control over the thickness of the deposited layer, which limits reproducible industrial production of PVs using these techniques. Moreover, both methods lead to films with nanometric size thicknesses.

Inkjet printing affords a strict control over the layer thickness. Additionally, there is no waste produced, and the required inks are simple low-viscosity formulations. PV cells with 11.3% of efficiency [92] have been accomplished using this approach. However, despite the roll-to-roll compatibility, clogging problems are quite common during the printing process, and therefore, efficient particle dispersion is of utmost importance to prevent damage to the equipment from the presence of agglomerations.

Screen printing is a very simple technique commonly used in the textile industry. It can be used to print active layers and produce devices on many different substrates, such as glass, polymer, textile, metal, and paper. The printed pattern is created by first placing a mesh above the chosen substrate (Fig. 5a), then with the use of a squeegee, the ink is spread through the mesh by applying pressure on it until the mesh touches the substrate. With a 45° angle between the squeegee and the mesh and a continuous pressure and velocity of the squeegee, the ink will pass through the mesh (Fig. 5b) and finally print the desired pattern on the substrate (Fig. 5c). A subsequent low-temperature treatment is performed to evaporate the solvent used in the ink formulation.

Recently, we embarked on the development of ink formulation for screen-printed fabrication of CIGS PVs. Notably, screen printing (Fig. 5) is the least explored of the techniques presented and the maximum efficiency achieved thus far for a screen-printed device is 6.1% [26]. Despite the need of a rheology additive to meet the high viscosity requirement, it is a very promising approach since it allows for the deposition of layers of large dimension with a good uniformity, high resolution, and low cost, rendering the technique very attractive for roll-to-roll industry. Furthermore, it is the most suitable technique to print layers with few micrometers of thickness, desirable for the CIGS layer. Although a low number of PV cells with screen-printed CIGS layer have been reported, the deposition is being optimized in both rigid [26,94] and flexible substrates [95,96].

Vacuum-based deposition processes are undoubtedly the most effective ones to achieve morphologically and compositionally uniform CIGS layers. Nonetheless, printing/solution-based processes are highly advantageous, both in terms of environmental impact and applicability of the devices. Although spin, spray, and blade coating are highly explored techniques in CIGS deposition, their implementation into roll-to-roll fabrication is impossible or challenging. Moreover, the low control over the layer thickness and the resultant very thin layers result in the need of repeating the print procedure several times to achieve the optimal CIGS layer thickness of 1–2.5 μm. Inkjet printing, on the other hand, despite providing a high control over the thickness, is a very complex technique that easily results in clogging problems in the nozzle and frequent equipment maintenance. Screen printing is facile, cheap, and very well-known in the industry. Therefore, it is a very promising technique for CIGS deposition, as it is compatible with roll-to-roll production and produces little material waste. For an all-sustainable procedure, the ink should be formulated using environmentally friendly solvents and nature-derived thickeners with low degradation temperatures to avoid high temperature procedures. Nevertheless, the mandatory high viscosity of the ink poses a challenge since an additional postdeposition procedure (e.g., thermal treatment) is necessary to remove the organic matter. The search and use of environmentally friendly viscous solvents with low molecular weight and low degradation temperature will allow to combat this limitation.

5.4. Current PVs

In the quest for solution-processed CIGS PVs, several reports have emerged using the printing/coating techniques for the CIGS layer. The most efficient CIGS PV cells are presented in Table 2, together with the nature of the precursors, ink formulation, and used post-deposition treatments. Currently, the most efficient PV cell (17.3%) comprising printed/solution-processed CIGS layer was developed using spin coating for CIGS deposition [61]. The second most efficient PV cell (15.0%) was
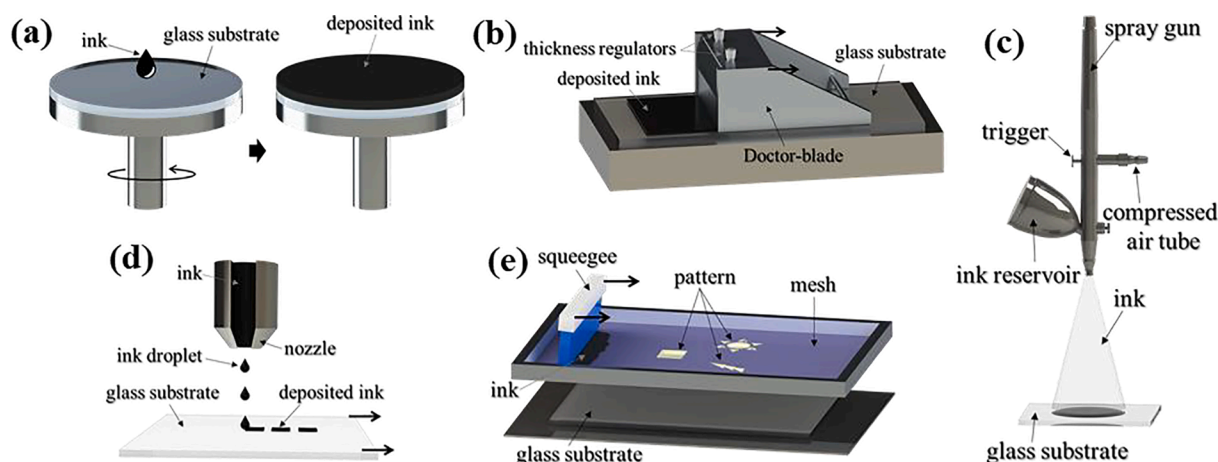

Fig. 4. Schematic representation of deposition techniques: (a) spin coating, (b) blade coating, (c) spray coating, (d) inkjet printing, and (e) screen printing.

Table 1

Comparison of the deposition techniques of the CIGS layer with main advantages, limitations, and characteristics [13,93]. The factors related to the sustainability associated with the CIGS PV fabrication are marked by color code, where red and green reflect high and low environmental/health impact, respectively.

|	Spin coating	Blade coating	Inkjet printing	Spray coating	Screen printing
Advantages	- Simple - Good control over thickness for small areas - Low cost	- Good stoichiometry control - Low cost	- Precise control over thickness and pattern - No mask needed	- Simple - Low cost - High throughput	- Simple - Low cost - Good control over thickness - High throughput
Limitations	- Low control over thickness for large areas	- Low control over thickness	- Difficult ink preparation (clogging) - High cost	- Low control over thickness	- Ink preparation (high viscosity)
Material waste	Significant	Little	None	Little	None
Wet thickness (µm)	1–200	10–200	0.5–5	5–200	10–100
Ink viscosity (cP)	<10	<10	<10	10–1000	100–100,000
Pattern resolution	Zero-dimensional	One-dimensional	Three-dimensional 16–50 µm	Zero-dimensional	Two-dimensional 30 µm
Roll-to-roll compatibility	No	Yes	Yes	Yes	Yes
Highest efficiency PV cell (%)	17.3 [61]	15.0 [72]	11.3 [93]	10.7 [92]	6.1 [26]
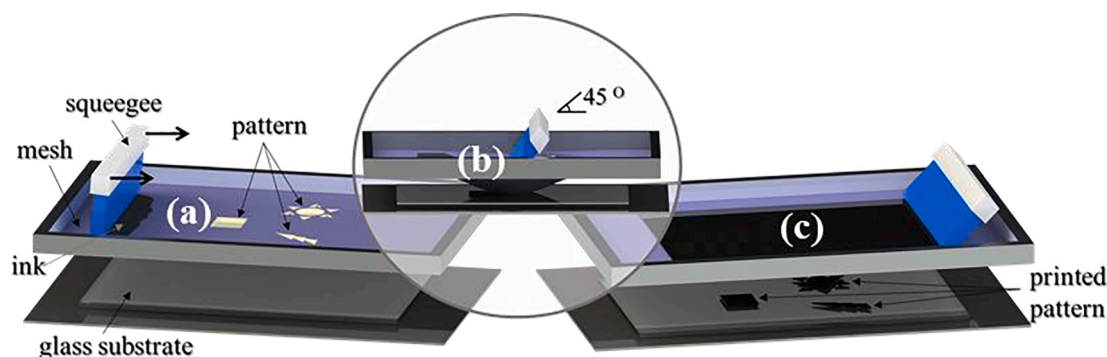
Fig. 5. The screen printing process steps and elements; (a) placement of the mesh with the printing pattern above the chosen substrate, (b) spread of the ink through the mesh by a squeegee, and (c) achievement of the printed pattern over the substrate.

Table 2

The most efficient and the most sustainable CIGS PV cells with a printed CIGS layer, with the corresponding precursor nature, ink formulation, and deposition process. The factors related to sustainability associated with the CIGS PV fabrication are marked by color code, where red and green reflect high and low environmental/health impact, respectively. The G score of the solvents, when available, are represented inside brackets.

Precursor nature			Ink formulation		Post-deposition treatment	Deposition process	Efficiency (%)	Ref.
Route	Chemicals	Solvent	Solvent	Additives				
Solution (molecular)	Cu$_2$S + In$_2$Se$_3$ + Ga + Se + S	Hydrazine	Hydrazine	---	Annealing 500–600 °C (N$_2$)	Spin coating	17.3	[61]
Particulate (hot injection synthesis)	Cu(acac)$_2$ + In(acac)$_3$ + Ga(acac)$_3$ + S	Oleyamine	Hexanethiol	---	Calcination 350 °C Selenization 500 °C	Blade coating	15.0	[72]
Solution (salts)	Cu(NO$_3$)$_2$·3H$_2$O + In(NO$_3$)$_3$·H$_2$O + Ga(NO$_3$)$_3$·H$_2$O	IPA (G = 6.5) + anhydrous ethylene glycol (G = 8.1)	IPA	Anhydrous ethylene glycol	Calcination 250 °C Two-step selenization 400 °C and 560 °C	Inkjet printing	11.3	[93]
Solution (salts)	Cu(NO$_3$)$_2$ + In(NO$_3$)$_3$ + Ga(NO$_3$)$_3$ + thiourea	Water (G = 7.3)	Water	Sodium nitrate	Annealing 330–360 °C (N$_2$) Selenization 560 °C	Spray coating	10.7	[92]
Particulate (commercial oxides)	CuO + In$_2$O$_3$ + Ga$_2$O$_3$ + oleic acid	D (propylene glycol) methyl ether	α-Terpineol	Ethyl cellulose	Calcination 100 °C and 400 °C Selenization 550 °C	Screen printing	6.1	[26]
Solution (salts)	Cu(NO$_3$)$_2$ + In(NO$_3$)$_3$ + Ga(NO$_3$)$_3$	Ethanol (G = 6.6)	Ethanol	---	Selenization 550 °C Sulfurization 550 °C	Spin coating	12.4	[81]
Solution (salts)	Cu(NO$_3$)$_2$ + In(NO$_3$)$_3$ + Ga(NO$_3$)$_3$	IPA + anhydrous ethylene glycol	IPA + anhydrous ethylene glycol	---	Calcination 250 °C Two-step selenization 400 °C and 560 °C	Inkjet printing	11.3	[93]
Particulate (synthesis-chemical ion reduction)	CuCl$_2$ + InCl$_3$ + GaCl$_3$ + SeCl$_4$ + NaBH$_4$	Polyethylene glycol	Ethanol + ethylene glycol	---	Annealing 450 °C (Ar)	Blade coating	9.3	[75]
Particulate (synthesis- sonochemical)	Cu(NO$_3$)$_2$ + In(NO$_3$)$_3$ + Ga(NO$_3$)$_3$ + triethanolamine + selenourea	Water	Water	---	Pulsed laser annealing with pulser fiber laser (1064 nm) under air at RT	Spray coating	1.1	[98]
Particulate-based (synthesis- sonochemical)	Cu(NO$_3$)$_2$ + In(NO$_3$)$_3$ + Ga(NO$_3$)$_3$ + triethanolamine + selenourea	Water	Ethanol	---	Flash-light (9 W in air at RT)	Spray coating	0.2	[99]

developed using blade coating for the CIGS layer [72]. Despite the high efficiencies, these procedures include the use of toxic or hazardous solvents, often even selenization, which is a hazardous process and non-suitable for roll-to-roll fabrication. Interestingly, only a few reports have emerged on screen printing, explaining its current lower efficiency (6.1%) [26]. Due to facile processability associated with screen printing, there is high potential for the use of this technique in the development of

CIGS PVs. Therefore, the development of screen printable inks comprising well-dispersed colloidal CIGS nanocrystals should be addressed to improve the performance of those devices.

Due to their toxicity, harmfulness, and damage to the environment, the replacement of hazardous organic solvents, such as hydrazine, toluene, and hexanethiol, in industrial processes is essential from the green chemistry and sustainability point of view. Green solvents are

environmentally friendly solvents derived from the processing of crops. In the search of environmentally friendly inks for the CIGS layer, iso-propanol (IPA) (G score = 6.5), ethanol (G score = 6.6), and water-based (G score = 7.3) inks have been identified. These sustainable alternatives to the solution-processed CIGS PV cells are also summarized in Table 2 and can be identified after the black horizontal line separating lines 5 and 6 from Table 2.

The search for sustainable and environmentally friendly approaches towards CIGS PV fabrication is ongoing, although the number of reports is still limited. As a step towards this direction, we successfully produced two eco-friendly inks with Cu, In, and Ga oxides dispersed in water/ethanol [99]. Nature-derived additives polyvinyl alcohol and hydrox-ypropyl methylcellulose were used to adjust the ink viscosities for screen-printing deposition over FTO-coated SLG. As the particulate-based ink method comprising commercial oxides demands further thermal treatment to incorporate selenium, RTA selenization was used to grow dense CIGS thin films with excellent crystallinity and morphology, ready to be employed in the sustainable production of a CIGS PV cell, which is currently ongoing.

In most examples of printed CIGS PV cells, the hazardous seleniza-tion treatment is employed during fabrication. However, a fully sus-tainable procedure must use environmentally friendly chemicals, solvents, and procedures from precursor synthesis, deposition, and post-deposition treatments to recycling and end-of-life. To avoid selenization, high-quality CIGS NPs can be directly incorporated into green particu-late ink formulations with further annealing the film without a Se source [75]. Notably, this strategy allowed for the production of a PV cell with 9.3% of efficiency. High-temperature annealing could be avoided using a method where the layer is crystallized using powerful lasers, which does not represent a danger to humans or the environment and is feasible for the roll-to-roll industry [97,98]. The use of low-temperature thermal annealing or alternative heatless processes will contribute not only to more sustainable procedures but also to preserve flexible sub-strates and allow the fabrication of flexible and versatile devices, and research efforts should be directed to these areas to advance the sus-tainability of the CIGS film printing.

5.5. Fully printed/solution-processed CIGS PVs

When implemented in roll-to-roll processing, printing technologies enable a much larger throughput than vacuum-based ones, increasing the development of flexible lightweight devices and their miniaturiza-tion, and expanding the devices field of application from space explo-ration to wearable devices. This field has been attracting much attention during the last decade, driving the development of fully printed devices in many different fields [100,101].

Combining printing techniques with the roll-to-roll process is of high benefit for the final cost of a PV cell. In addition, the amount of waste products and the energy demand are lower than for vacuum-processed devices, resulting in a more sustainable PV cell production. A few fully solution-processed PV cells have been recently developed [102-105] and currently, their major limitation lies in the low efficiency, mostly stemming from the photoabsorber layer (e.g. gallium segrega-tion, recombination centers, grain boundaries). As an example, a fully printed CuInS$_2$ chalcogenide PV cell delivered a maximum efficiency of 7.2% [106 103].

Very few examples of fully solution-processed CIGS PVs have been reported. Nagino et al. [107] reported the one with the highest effi-ciency of 10.9%. It comprises an FTO back contact spray-coated over SLG and a spin-coated CIGS layer, with a final annealing and seleniza-tion at 550 °C to grow the crystal. However, no specification about the precursors' nature, ink formulation, or used deposition process is re-ported. Thereafter, a CdS layer deposited by chemical bath and ZnO NPs, working as a high-resistance buffer, and Ag nanowires (NWs), working as a transparent front contact, were sequentially spin coated. Finally, Ag grid electrodes were screen printed on top of Ag NWs.

Another fully solution-processed CIGS PV cell showed an efficiency of 1.6% [108]. CIGS NPs synthesized in dodecylamine were suspended in o-dichlorobenzene to produce a spin-coating ink deposited over Mo-coated glass, which was further annealed without the need of seleniza-tion. Next, the CdS buffer and a conductive layer of sol−gel derived ZnO precursor solution, comprising 2-methoxyethanol and monoethanl-amine solvents, were spin-coated sequentially. Finally, AgNWs were spin-coated over the ZnO layer, and finally, another ZnO layer was spin-coated on top, requiring final annealing of 200 °C. The authors attribute the low efficiency of the device to the poor quality of the photoabsorber film. More specifically, the low CIGS particle size (20 nm) results in a partly dense film that increases the potential recombination of charge carries, and therefore decreases the photovoltaic performance.

The limited efficiency given by fully printed/solution-processed PV cells typically stems from the CIGS photoabsorber layer deposition [109]. While the search for more effective printed CIGS layers is ongoing, improvements have been achieved on the buffer and front contact layers. Regarding the CdS buffer layer, chemical bath deposition is a well-established method used in high-efficiency CIGS PV cells [110]. Although it is a non-vacuum deposition process, the toxicity of Cd has driven the search for greener alternatives [19].

Printable transparent front contacts, on the contrary, have been extensively investigated. In addition to the basic requirements of high transmittance and conductivity, the maximum processing temperature should not exceed 220 °C; otherwise, the layers below will be compro-mised. There are several candidates fulfilling these requirements, such as conductive polymers, carbon allotropes, and metal NWs [111]. Printable front contacts have been developed to be implemented in CIGS PV cells with vacuum-deposited CIGS layer to replace the commonly used vacuum-deposited ZnO and ZnO:Al layers (Table 3).

Although vacuum deposition is the most effective way to produce high-quality top conductive layers, printed/solution-processing is a more sustainable and affordable alternative. From the examples re-ported thus far, AgNWs are a viable solution to complete the CIGS PV cell fabrication process due to their excellent optical and electrical properties as well as low-temperature deposition. Due to the low thicknesses required for top conductive layers (~400 nm), spray coating is the best option, as it is simple, cheap, compatible with roll-to-roll production, and does not demand the use of thickeners, therefore avoiding the use of high-temperature annealing treatments. Notably, environmentally friendly ink formulations for top conductive layers have been developed. The combination of printed and sustainable top conductive layers with the printed/coated and sustainable CIGS layers will allow the production of cost-effective and sustainable all-printed/solution-processed CIGS PVs.

6. Future prospects

Importantly, printed PVs have been following a path where the ef-ficiencies are being optimized to compete with vacuum-based technol-ogy. To this end, efforts are being placed on improved metal dispersion, controllable deposition processes, uniformly printed films, and controlled film growth to obtain the desirable dense CIGS layers with improved PV performance. At the same time, environmentally friendly alternatives to the hazardous solvents used in ink formulations are being employed and the resultant inks are being successfully deposited by different techniques to produce CIGS PV cells (Fig. 6a). On the other hand, TCO inks comprising environmentally friendly solvents have been developed and coated by different techniques to complete the CIGS PV devices (Fig. 6a). These recent advances combined with the societal-environmental concerns will set out a trend for the future production of environmentally friendly all-solution-processed PV devices.

Nevertheless, most of the current studies comprising environmen-tally friendly solvents use the hazardous selenization treatment to finish the CIGS layer (Fig. 6b). To overcome this, alternatives to selenization are being developed. However, the use of environmentally friendly

Table 3

Printed conductive transparent top layers (first layers on the left) used in CIGS PV cell development and their sheet resistance (R_S), transmittance at 550 nm (T_{550nm}), and the reported efficiency. The factors related to sustainability associated with the CIGS PV fabrication are marked by color code, where red and green reflect high and low environmental/health impact, respectively. The G score of the solvents, when available, are represented inside brackets. (See below-mentioned references for further information.)

PV cell configuration	Ink formulation		Post-deposition treatment	Deposition process	R_S (Ω/sq)	T_{550nm} (%)	Efficiency (%)	Ref.
	Solvent	Additives						
SWCNT/ i-ZnO/CdS/CIGS/Mo/SLG	Water (G = 7.3) + non-specified alcohol	---	No information	Spray coating	50	78	19.5	[113]
AgNWs/ZnO:Al/ i-ZnO/CdS/CIGS/Mo/SLG	ZnO:Al: Ethanol (G = 6.6) + methoxyethanol (G = 4.3) AgNWs: ethanol	ZnO:Al: Ethanolamine	Annealing 180 °C Calcination 200 °C	Spray coating	20	92	14.1	[112]
ZnO/AgNWs/ZnO/ CdS/CIGS/Mo/SLG	ZnO: 2-methoxyethanol + monoethanolamine AgNWs: Ethanol	---	Calcination 70 °C and 150 °C	Spin coating	11	90	13.5	[114]
AgNWs+PEDOT:PSS/ Zn(S,O,OH)/CdS/CIGS/ Mo/SLG	AgNWs: Methanol (G = 5.8) PEDOT:PSS: Dimethyl sulfoxide (G = 6.4)	---	RTA (no *T* information)	Spray and spin coating	12	82	11.6	[115]
ZnO:Al/AgNWs/ZnO:Al/ i-ZnO/CdS/CIGS/Mo/SLG	ZnO:Al: 2-methoxyethanol AgNWs: IPA	ZnO:Al: Ethanolamine + Formamide (G = 5.5)	Calcination 150 °C Annealing 200 °C Ultraviolet-ozone treatment	Spin coating	11	93	11.0	[116]
AgNWs-ITO NP/ ZnS/CIGS/Mo/SLG	AgNWs: IPA (G = 6.5) ITO NP: IPA + Water	ITO NP: Polyvinyl alcohol	Annealing 100 °C	Spin coating	23	87	8.0	[117]

solvents with appropriate polarity, viscosity, and surface tension to disperse metal particles, as well as the absence of selenization treatment to grow the CIGS crystal to produce high-efficiency PV devices is very challenging. To this end, we highlight a recent study reporting a PV device with >9% of efficiency produced using an ethanol-based ink and avoiding a selenization step by using synthesized CIGS NPs [75], overcoming the low efficiency usually associated with sustainable alternative devices. The stabilization of the NPs with polyethylene glycol and the presence of a uniform cluster size of the NPs between 100 and 200 nm contributed to the exciting result. Thus far, using synthetic CIGS NPs, the best-performing devices involve the use of high-temperature syntheses and photoabsorber layers with thicknesses under 1.5 μm (Fig. 6c).

Recently, efforts in obtaining sustainable all-solution-processed PV devices with more satisfactory performance have given access to performances up to 10.9% of efficiency. Importantly, all procedures should be designed with recycling strategies envisioned since the beginning and considering the respective techno-economic and life-cycle assessments. To continue the pursuit for sustainable all-solution-processed CIGS PVs, environmentally friendly synthesis of high-quality CIGS NPs is desirable. Moreover, CIGS NPs well dispersed in ink formulations comprising green solvents and chemicals, with low organic content, and uniform deposition for compact thin films can be a solution since it avoids the need for a selenization step. The critical factors are the grain size and size distribution of the nanocrystals. The design of sustainable colloidal synthetic procedures to deliver nanosized and homogeneous CIGS crystals, as well as fine dispersion of the nanocrystals into inks tailored towards screen printing, are the next milestones to surpass the film defects. Alternatively, if the use of organic compounds as stabilizer or in the ink formulation cannot be avoided, the use of nature-derived chemicals with low degradation temperature should be targeted. Afterwards, to degrade the organic matter, low-temperature annealing or laser technologies present a solution to avoid high-temperature annealing temperatures that prevent the use of flexible substrates. Finally, as top contact to complete the PV devices, spray-coated nanometric layers comprising environmentally friendly inks with well-dispersed AgNWs could lead to cost-efficient and sustainable all-solution-processed CIGS PV devices.

There is a clear tendency in the upcoming years for the use of environmentally friendly inks in combination with non-vacuum deposition processes, compatible with roll-to-roll industry, and soft or alternative thermal processes to produce fully printed/solution-processed and sustainable CIGS PVs. The continuous research in this direction has the potential to bring this technology to a higher commercially competitive path with major gains in the flexibility and the range of applicability of these devices, as well as meeting the societal and governmental goals for improved sustainability of materials, processes, and applications.

7. Conclusions

The PV market has been growing and providing solutions beyond the silicon technology. Second generation thin-film PV cells have been attracting a lot of attention and great advances have been made in CIGS, which recently reached 23.35% of efficiency. In the industry, this type of PV cells are currently fabricated by vacuum-based deposition techniques, and these methods have become increasingly powerful and versatile as a result of innovations in the area. Despite affording high-performing CIGS PV modules, the processes used in vacuum-based fabrication are typically unsustainable and sometimes toxic to humans/environment.

The high demand for sustainable and environmentally benign fabrication methods of CIGS PVs has prompted an active search for low-cost alternatives to vacuum-deposition processes. To address the trend, this review focused on printed/solution-processed CIGS PV cells, presenting an up-to-date summary of recent efforts that couple eco-friendly inks and cost-efficient non-vacuum deposition techniques. As a result, greener PV cells have been developed, which to date present ca. 30% lower efficiencies than those fabricated by vacuum deposition. Looking forward, the continuous search for efficient "green" CIGS inks and suitable printing processes is very important and will lead these PVs to a more competitive path.

The printable technology market is growing, producing printed devices for many different fields of application that can be placed anywhere, even in the human body. Fully printed/solution-processed CIGS PV cells remain scarce. However, they present a major advantage in terms of price, miniaturization, flexibility, weight, and especially
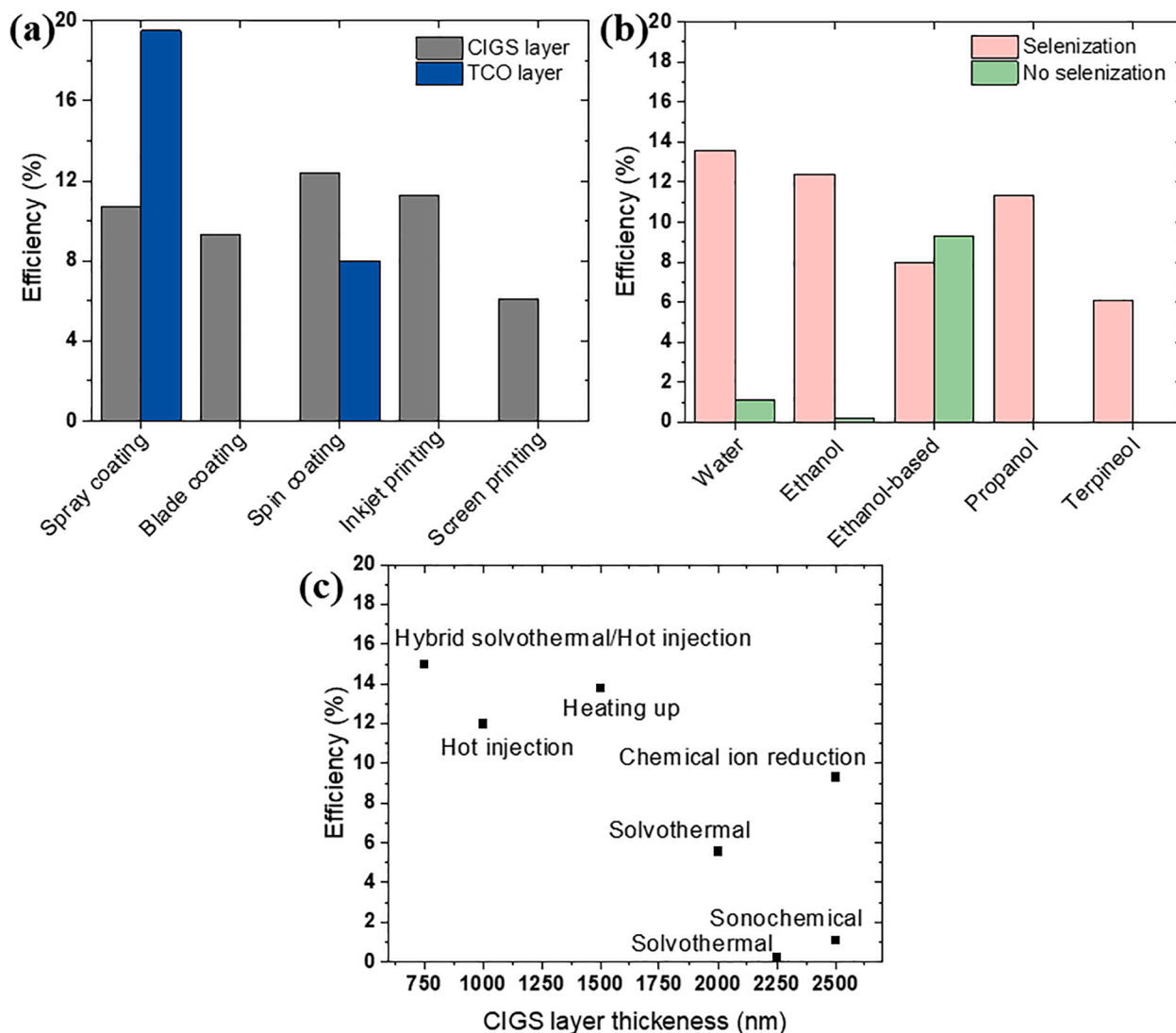
Fig. 6. CIGS PV cells efficiencies using (a) environmentally friendly ink formulations and non-vacuum-based deposition of CIGS (grey) and TCO (blue) layers, (b) ink formulations for CIGS layer comprising environmentally friendly solvents with further selenization thermal treatment (red) and without selenization (green), and (c) synthesized CIGS NPs produced by different synthetic methods and using different photoabsorber layer thicknesses. (For interpretation of the references to color in this figure legend, the reader is referred to the web version of this article.)

expanding fields of application, such as windows and textiles. In the case of printed CIGS PVs, the reported evidences suggest that the harsh selenization step is limiting and must be eliminated. Hence, the formulation of improved CIGS NP inks and their printing protocols are projected to play a significant and enabling role in omitting the selenization obstacle during sustainable fabrication of CIGS PVs, thus strongly aiding the urgently needed clean energy transition. The development of (*i*) tunable, large-scale aqueous syntheses of high-quality NPs (phase-pure, highly crystalline, desired physical properties) of key constituent materials of CIGS PVs (Fig. 2a), (*ii*) the formulation of the respective green inks (NPs + green solvents + bio-based additives) with excellent rheological properties, and (*iii*) extensive implication of industrially-relevant coating/printing deposition in PV fabrication will likely be crucial targets of the future efforts.

CRediT authorship contribution statement

Bruna F. Gonçalves: Writing – original draft. **Sascha Sadewasser:** Writing – review & editing. **Laura M. Salonen:** Writing – review & editing. **Senentxu Lanceros-Méndez:** Writing – review & editing, Supervision, Funding acquisition. **Yury V. Kolen'ko:** Writing – review &

editing, Supervision, Funding acquisition.

Declaration of Competing Interest

The authors declare that they have no known competing financial interests or personal relationships that could have appeared to influence the work reported in this paper.

Acknowledgement

References

[1] S.J. Davis, N.S. Lewis, M. Shaner, S. Aggarwal, D. Arent, I.L. Azevedo, S. M. Benson, T. Bradley, J. Brouwer, Y.-M. Chiang, C.T.M. Clack, A. Cohen, S. Doig, J. Edmonds, P. Fennell, C.B. Field, B. Hannegan, B.-M. Hodge, M.I. Hoffert, E. Ingersoll, P. Jaramillo, K.S. Lackner, K.J. Mach, M. Mastrandrea, J. Ogden, P. F. Peterson, D.L. Sanchez, D. Sperling, J. Stagner, J.E. Trancik, C.-J. Yang, K. Caldeira, Net-zero emissions energy systems, Science 360 (6396) (2018) eaas9793, https://doi.org/10.1126/science.aas9793.

[2] United Nations/Framework Convention on Climate Change, Decision 1/CP.21 Adoption of the Paris Agreement, 21st Conference of the Parties, Paris, United Nations, 2015.

[3] European Comission, Communication from the comission to the european parliament, the european council, the council, the european economic and social commitee and the commitee of the regions: The European Green Deal, COM 640 final, 2019.

[4] J.A. Luceño-Sánchez, A.M. Díez-Pascual, R. Peña Capilla, Materials for photovoltaics: state of art and recent developments, Int. J. Mol. Sci. 20 (4) (2019) 976, https://doi.org/10.3390/ijms20040976.

[5] C. Mustansar, Chapter 41 - Engineered Nanomaterials for Energy Applications, in: C. Mustansar (Ed.), Handbook of Nanomaterials for Industrial Applications, Elsevier2018, pp. 751-767. 10.1016/B978-0-12-813351-4.00043-2.

[6] I. Celik, M. Lunardi, A. Frederickson, R. Corkish, Sustainable end of life management of crystalline silicon and thin film solar photovoltaic waste: the impact of transportation, Appl. Sci. 10 (16) (2020) 5465, https://doi.org/10.3390/app10165465.

[7] M. Tawalbeh, A. Al-Othman, F. Kafiah, E. Abdelsalam, F. Almomani, M. Alkasrawi, Environmental impacts of solar photovoltaic systems: A critical review of recent progress and future outlook, Sci. Total Environ. 759 (2021), 143528, https://doi.org/10.1016/j.scitotenv.2020.143528.

[8] J.P.A.-G. M. M. Lunardi, J. I. Bilbao and R. Corkish, A Review of Recycling Processes for Photovoltaic Modules, Solar Panels and Photovoltaic Materials, IntechOpen2018. 10.5772/intechopen.74390.

[9] S. Wagner, J.L. Shay, P. Migliorato, H.M. Kasper, CuInSe$_2$/CdS heterojunction photovoltaic detectors, Appl. Phys. Lett. 25 (8) (1974) 434–435, https://doi.org/10.1063/1.1655537.

[10] M. Contreras, J. Tuttle, D. Du, Y. Qi, A. Swartzlander, A. Tennant, R. Noufi, Graded band-gap Cu(In, Ga)Se$_2$ thin-film solar cell absorber with enhanced open-circuit voltage, Appl. Phys. Lett. 63 (13) (1993) 1824–1826, https://doi.org/10.1063/1.110675.

[11] CIGS White Paper 2019, 2019. https://cigs-pv.net/wortpresse/wp-content/uploads/2019/04/CIGS_White_Paper_2019_online.pdf, accessed on February 2021.

[12] S. Koebrich, T. Bowen, A. Sharpe, Renewable Energy Data Book, U.S. Department of Energy, 2020.

[13] J. Ramanujam, U.P. Singh, Copper indium gallium selenide based solar cells – a review, Energy Environ. Sci. 10 (6) (2017) 1306–1319, https://doi.org/10.1039/C7EE00826K.

[14] M. Kemell, M. Ritala, M. Leskelä, Thin Film Deposition Methods for CuInSe$_2$ Solar Cells, Crit. Rev. Solid State Mater. Sci. 30 (1) (2005) 1–31, https://doi.org/10.1080/10408430590918341.

[15] N. Mufti, T. Amrillah, A. Taufiq, Sunaryono, Aripriharta, M. Diantoro, Zulhadjri, H. Nur, Review of CIGS-based solar cells manufacturing by structural engineering, Solar Energy 207 207 (2020) 1146–1157.

[16] U. Rau, H.W. Schock, Chapter IC-3 - Cu(In,Ga)Se$_2$ Thin-Film Solar Cells, in: A. McEvoy, T. Markvart, L. Castañer (Eds.), Practical Handbook of Photovoltaics (2nd Edition), Academic Press, Boston, 2012, pp. 323-371. 10.1016/B978-0-12-385934-1.00010-6.

[17] S. Rühle, Tabulated values of the Shockley-Queisser limit for single junction solar cells, Sol. Energy 130 (2016) 139–147, https://doi.org/10.1016/j.solener.2016.02.015.

[18] J.-F. Guillemoles, T. Kirchartz, D. Cahen, U. Rau, Guide for the perplexed to the Shockley-Queisser model for solar cells, Nat. Photonics 13 (8) (2019) 501–505, https://doi.org/10.1038/s41566-019-0479-2.

[19] M. Nakamura, K. Yamaguchi, Y. Kimoto, Y. Yasaki, T. Kato, H. Sugimoto, Cd-Free Cu(In, Ga)(Se,S)$_2$ Thin-Film Solar Cell With Record Efficiency of 23.35%, IEEE J. Photovolt. 9 (2019) 1863–1867, https://doi.org/10.1109/JPHOTOV.2019.2937218.

[20] M. Green, E. Dunlop, J. Hohl-Ebinger, M. Yoshita, N. Kopidakis, X. Hao, Solar cell efficiency tables (version 57), Prog. Photovolt. Res. Appl. 29 (1) (2021) 3–15, https://doi.org/10.1002/pip.3371.

[21] C.A. Kaufmann, A. Neisser, R. Klenk, R. Scheer, Transfer of Cu(In, Ga)Se$_2$ thin film solar cells to flexible substrates using an in situ process control, Thin Solid Films 480–481 (2005) 515–519, https://doi.org/10.1016/j.tsf.2004.11.067.

[22] Y. Kawano, J. Chantana, T. Nishimura, A. Mavlonov, T. Minemoto, Manipulation of [Ga]/([Ga]+[In]) profile in 1.4-μm-thick Cu(In, Ga)Se$_2$ thin film on flexible stainless steel substrate for enhancing short-circuit current density and conversion efficiency of its solar cell, Sol. Energy 204 (2020) 231–237, https://doi.org/10.1016/j.solener.2020.04.069.

[23] A. Chirilă, S. Buecheler, F. Pianezzi, P. Bloesch, C. Gretener, A.R. Uhl, C. Fella, L. Kranz, J. Perrenoud, S. Seyrling, R. Verma, S. Nishiwaki, Y.E. Romanyuk, G. Bilger, A.N. Tiwari, Highly efficient Cu(In, Ga)Se$_2$ solar cells grown on flexible polymer films, Nat. Mater. 10 (11) (2011) 857–861, https://doi.org/10.1038/nmat3122.

[24] A. Reinders, P. Verlinden, W. van Sark, A. Freundlich, Chapter 4 - Basics of chalcogenide thin film solar cells, Photovoltaic Solar Energy: From Fundamentals to Applications, Wiley2017, pp. 169-212.

[25] Y. Li, G. Yin, Y. Gao, T. Köhler, J. Lucaßen, M. Schmid, Sodium control in Ultrathin Cu(In, Ga)Se$_2$ solar cells on transparent back contact for efficiencies beyond 12%, Sol. Energy Mater. Sol. Cells 223 (2021), 110969 https://doi.org/10.1016/j.solmat.2021.110969.

[26] V. Sousa, B.F. Gonçalves, Y.S. Rosen, J. Virtuoso, P. Anacleto, M.F. Cerqueira, E. Modin, P. Alpuim, O.I. Lebedev, S. Magdassi, S. Sadewasser, Y.V. Kolen'ko, Over 6% Efficient Cu(In,Ga)Se$_2$ Solar Cell Screen-Printed from Oxides on Fluorine-Doped Tin Oxide, ACS Appl. Energy Mater. 3(4) (2020) 3120-3126. 10.1021/acsaem.9b01999.

[27] M. Saifullah, D. Kim, J.-S. Cho, S. Ahn, S. Ahn, J.H. Yun, H.S. Lee, J.H. Park, The role of NaF post-deposition treatment on the photovoltaic characteristics of semitransparent ultrathin Cu(In, Ga)Se$_2$ solar cells prepared on indium-tin-oxide back contacts: a comparative study, J. Mater. Chem. A 7 (38) (2019) 21843–21853, https://doi.org/10.1039/C9TA06274B.

[28] L. Gouillart, A. Cattoni, J. Goffard, F. Donsanti, G. Patriarche, M. Jubault, N. Naghavi, S. Collin, Development of reflective back contacts for high-efficiency ultrathin Cu(In, Ga)Se$_2$ solar cells, Thin Solid Films 672 (2019) 1–6, https://doi.org/10.1016/j.tsf.2018.12.041.

[29] G. Regmi, A. Ashok, P. Chawla, P. Semalti, S. Velumani, S.N. Sharma, H. Castaneda, Perspectives of chalcopyrite-based CIGSe thin-film solar cell: a review, J. Mater. Sci.: Mater. Electron. 31 (10) (2020) 7286–7314, https://doi.org/10.1007/s10854-020-03338-2.

[30] B. Vermang, J.T. Wätjen, C. Frisk, V. Fjällström, F. Rostvall, M. Edoff, P. Salomé, J. Borme, N. Nicoara, S. Sadewasser, Introduction of Si PERC Rear Contacting Design to Boost Efficiency of Cu(In, Ga)Se$_2$ Solar Cells, IEEE J. Photovoltaics 4 (6) (2014) 1644–1649, https://doi.org/10.1109/JPHOTOV.2014.2350696.

[31] P. Casper, R. Hünig, G. Gomard, O. Kiowski, C. Reitz, U. Lemmer, M. Powalla, M. Hetterich, Optoelectrical improvement of ultra-thin Cu(In,Ga)Se$_2$ solar cells through microstructured MgF$_2$ and Al$_2$O$_3$ back contact passivation layer, Physica Status Solidi – Rapid Research Letters 10(5) (2016) 376-380. 10.1002/pssr.201600018.

[32] G. Yin, M. Song, S. Duan, P. Manley, D. Greiner, C.A. Kaufmann, M. Schmid, Well-Controlled Dielectric Nanomeshes by Colloidal Nanosphere Lithography for Optoelectronic Enhancement of Ultrathin Cu(In, Ga)Se$_2$ Solar Cells, ACS Appl. Mater. Interfaces 8 (46) (2016) 31646–31652, https://doi.org/10.1021/acsami.6b10135.

[33] C. van Lare, G. Yin, A. Polman, M. Schmid, Light Coupling and Trapping in Ultrathin Cu(In, Ga)Se$_2$ Solar Cells Using Dielectric Scattering Patterns, ACS Nano 9 (10) (2015) 9603–9613, https://doi.org/10.1021/acsnano.5b04091.

[34] G. Yin, V. Brackmann, V. Hoffmann, M. Schmid, Enhanced performance of ultra-thin Cu(In, Ga)Se$_2$ solar cells deposited at low process temperature, Sol. Energy Mater. Sol. Cells 132 (2015) 142–147, https://doi.org/10.1016/j.solmat.2014.08.045.

[35] M.A. Mughal, R. Engelken, R. Sharma, Progress in indium (III) sulfide (In$_2$S$_3$) buffer layer deposition techniques for CIS, CIGS, and CdTe-based thin film solar cells, Sol. Energy 120 (2015) 131–146, https://doi.org/10.1016/j.solener.2015.07.028.

[36] S. Hwang, L. Larina, H. Lee, S. Kim, K.S. Choi, C. Jeon, B.T. Ahn, B. Shin, Wet Pretreatment-Induced Modification of Cu(In, Ga)Se$_2$/Cd-Free ZnTiO Buffer Interface, ACS Appl. Mater. Interfaces 10 (24) (2018) 20920–20928, https://doi.org/10.1021/acsami.8b01090.

[37] J. Chantana, T. Kato, H. Sugimoto, T. Minemoto, 20% Efficient Zn$_{0.9}$Mg$_{0.1}$O:Al/Zn$_{0.8}$Mg$_{0.2}$O/Cu(In,Ga)(S,Se)$_2$ Solar Cell Prepared by All-Dry Process through a Combination of Heat-Light-Soaking and Light-Soaking Processes, ACS Applied Materials & Interfaces 10(13) (2018) 11361-11368. 10.1021/acsami.8b01247.

[38] K.S. Gour, P. Parmar, R. Kumar, V.N. Singh, Cd-Free Zn(O, S) as Alternative Buffer Layer for Chalcogenide and Kesterite Based Thin Films Solar Cells: A Review, J. Nanosci. Nanotechnol. 20 (6) (2020) 3622–3635, https://doi.org/10.1166/jnn.2020.17537.

[39] M. Powalla, S. Paetel, D. Hariskos, R. Wuerz, F. Kessler, P. Lechner, W. Wischmann, T.M. Friedlmeier, Advances in Cost-Efficient Thin-Film Photovoltaics Based on Cu(In, Ga)Se$_2$, Engineering 3 (4) (2017) 445–451, https://doi.org/10.1016/J.ENG.2017.04.015.

[40] A. Kumar, A. Kumar Goyal, U. Gupta, N. Tanya, R.C. Gupta, Increased efficiency of 23% for CIGS solar cell by using ITO as front contact, Mater. Today:. Proc. 28 (2020) 361–365, https://doi.org/10.1016/j.matpr.2020.02.688.

[41] T. Minemoto, J. Julayhi, Buffer-less Cu(In, Ga)Se$_2$ solar cells by band offset control using novel transparent electrode, Curr. Appl Phys. 13 (1) (2013) 103–106, https://doi.org/10.1016/j.cap.2012.06.019.

[42] Y. Kuwahata, T. Minemoto, Impact of Zn$_{1-x}$Mg$_x$O: Al transparent electrode for buffer-less Cu(In, Ga)Se$_2$ solar cells, Renewable Energy 65 (2014) 113–116, https://doi.org/10.1016/j.renene.2013.07.038.

[43] A.E. Delahoy, L. Chen, M. Akhtar, B. Sang, S. Guo, New technologies for CIGS photovoltaics, Sol. Energy 77 (6) (2004) 785–793, https://doi.org/10.1016/j.solener.2004.08.012.

[44] T. Jäger, Y.E. Romanyuk, S. Nishiwaki, B. Bissig, F. Pianezzi, P. Fuchs, C. Gretener, M. Döbeli, A.N. Tiwari, Hydrogenated indium oxide window layers for high-efficiency Cu(In, Ga)Se$_2$ solar cells, J. Appl. Phys. 117 (20) (2015), 205301, https://doi.org/10.1063/1.4921445.

[45] A. Klein, Energy band alignment in chalcogenide thin film solar cells from photoelectron spectroscopy, J. Phys.: Condens. Matter 27 (13) (2015), 134201, https://doi.org/10.1088/0953-8984/27/13/134201.

[46] L. Mansfield, Manufacturing and Reliability Science of CIGS Photovoltaics, Golden, CO: National Renewable Energy Laboratory (NREL/TP-5K00-72953) (2019).

[47] M. Theelen, F. Daume, Stability of Cu(In, Ga)Se₂ solar cells: A literature review, Sol. Energy 133 (2016) 586–627, https://doi.org/10.1016/j.solener.2016.04.010.

[48] P. Wolfram, Method for recycling a thin layer solar module during simultaneous recovering of recyclable material, by loading photovoltaic cells to be processed so that the plastic portion is separated from remaining components of the module, Loser Chemie, Germany, 2008, p. DE102008058530A1.

[49] M.S. Chowdhury, K.S. Rahman, T. Chowdhury, N. Nuthammachot, K. Techato, M. Akhtaruzzaman, S.K. Tiong, K. Sopian, N. Amin, An overview of solar photovoltaic panels' end-of-life material recycling, Energy Strategy Reviews 27 (2020), 100431, https://doi.org/10.1016/j.esr.2019.100431.

[50] V.K. Kapur, M. Fisher, R. Roe, Nanoparticle Oxides Precursor Inks for Thin film Copper Indium Gallium Selenide (CIGS) Solar Cells, MRS Proceedings 668 (2011) H2.6, https://doi.org/10.1557/PROC-668-H2.6.

[51] Sustainable Development Solutions Network: A Global Initiative for the United Nations, Mapping the Renewable Energy Sector to the Sustainable Development Goals: An Atlas, 2019.

[52] C.J. Clarke, W.-C. Tu, O. Levers, A. Bröhl, J.P. Hallett, Green and Sustainable Solvents in Chemical Processes, Chem. Rev. 118 (2) (2018) 747–800, https://doi.org/10.1021/acs.chemrev.7b00571.

[53] United Nations, Globaly Harmonized System of Classification and Labelling of Chemicals (GSH), New York and Geneva, United Nations, 2011.

[54] C.M. Alder, J.D. Hayler, R.K. Henderson, A.M. Redman, L. Shukla, L.E. Shuster, H. F. Sneddon, Updating and further expanding GSK's solvent sustainability guide, Green Chem. 18 (13) (2016) 3879–3890, https://doi.org/10.1039/C6GC00611F.

[55] C. Larsen, P. Lundberg, S. Tang, J. Ràfols-Ribé, A. Sandström, E. Mattias Lindh, J. Wang, L. Edman, A tool for identifying green solvents for printed electronics, Nature, Communications 12 (1) (2021) 4510, https://doi.org/10.1038/s41467-021-24761-x.

[56] B. Bakhiyi, F. Labrèche, J. Zayed, The photovoltaic industry on the path to a sustainable future — Environmental and occupational health issues, Environ. Int. 73 (2014) 224–234, https://doi.org/10.1016/j.envint.2014.07.023.

[57] R. Yang, E. Mazalan, K.T. Chaudhary, Z. Haider, J. Ali, Non-vacuum deposition methods for thin film solar cell: Review, AIP Conf. Proc. 1824 (1) (2017) 030018, https://doi.org/10.1063/1.4978836.

[58] NEXCIS Achieves a New Record Performance @ 17.3% Certified Pixel Measurement with its CIGS PV Technology, 2014. www.nexcis.fr (accessed 2021-07-01).

[59] M. Kaelin, D. Rudmann, A.N. Tiwari, Low cost processing of CIGS thin film solar cells, Sol. Energy 77 (6) (2004) 749–756, https://doi.org/10.1016/j.solener.2004.08.015.

[60] G. Brown, P. Stone, J. Woodruff, B. Cardozo, D. Jackrel, Device characteristics of a 17.1% efficient solar cell deposited by a non-vacuum printing method on flexible foil, 2012 38th IEEE Photovoltaic Specialists Conference, 2012, pp. 003230-003233.

[61] T. Zhang, Y. Yang, D. Liu, S.C. Tse, W. Cao, Z. Feng, S. Chen, L. Qian, High Efficiency Solution-Processed Thin-Film Cu(In, Ga)(Se, S)₂ Solar Cells, Energy Environ. Sci. 9 (12) (2016) 3674–3681, https://doi.org/10.1039/C6EE02352E.

[62] Y. Liu, D. Kong, Synthesis and characteristics of Cu(In, Ga)Se₂ thin films from nanoparticles by solvothermal method and selenisation process, Micro Nano Lett. 7 (11) (2012) 1112–1116, https://doi.org/10.1049/mnl.2012.0615.

[63] Y.T.C. Báez, D.A.F. Peña, J.A. Gómez-Cuaspud, E. Vera-López, Y. Pineda-Triana, Hydrothermal synthesis of a photovoltaic material based on CuIn₀.₅Ga₀.₅Se₂, J. Phys.: Conference Series 935 (2017), 012004, https://doi.org/10.1088/1742-6596/935/1/012004.

[64] M. Latha, R. Aruna Devi, S. Velumani, Hot injection synthesis of Cu(In, Ga)Se₂ nanocrystals with tunable bandgap, Opt. Mater. 79 (2018) 450–456, https://doi.org/10.1016/j.optmat.2018.04.016.

[65] V. Sousa, B.F. Gonçalves, M. Franco, Y. Ziouani, N. González-Ballesteros, M. Fátima Cerqueira, V. Yannello, K. Kovnir, O.I. Lebedev, Y.V. Kolen'ko, Superstructural Ordering in Hexagonal CuInSe₂ Nanoparticles, Chemistry of Materials 31(1) (2019) 260-267. 10.1021/acs.chemmater.8b04368.

[66] B.F. Gonçalves, A.P. LaGrow, S. Pyrlin, B. Owens-Baird, G. Botelho, L.S. A. Marques, M.M.D. Ramos, K. Kovnir, S. Lanceros-Mendez, Y.V. Kolen'ko, Large-Scale Synthesis of Semiconducting Cu(In, Ga)Se₂ Nanoparticles for Screen Printing Application, Nanomaterials 11 (5) (2021) 1148, https://doi.org/10.3390/nano11051148.

[67] M. Rohini, P. Reyes, S. Velumani, M. Latha, G. Oza, I. Becerril-Juarez, R. Asomoza, Parametric optimization of mechanochemical process for synthesis of Cu(In, Ga)₀.₅Se₂ nanoparticles, Mater. Sci. Semicond. Process. 37 (2015) 151–158, https://doi.org/10.1016/j.mssp.2015.02.046.

[68] J.-H. Cha, S.J. Noh, D.-Y. Jung, Synthesis and Nanostructures of Metal Selenide Precursors for Cu(In, Ga)Se₂ Thin-Film Solar Cells, ChemSusChem 8 (14) (2015) 2407–2413, https://doi.org/10.1002/cssc.201403464.

[69] K.P. Mubiayi, J. Freitas, M.J. Moloto, N. Moloto, L.M. Sikhwivhilu, A.F. Nogueria, Colloidal synthesis of CuIn₀.₇₅Ga₀.₂₅Se₂ nanoparticles and their photovoltaic performance, 14(1) (2016) 420. 10.1515/phys-2016-0046.

[70] M. Latha, R. Aruna-Devi, S. Velumani, B. Murali, J. Santoyo-Salazar, F. de Moure-Flores, Solution based synthesis of Cu(In, Ga)Se₂ microcrystals and thin films, RSC Adv. 9 (60) (2019) 35197–35208, https://doi.org/10.1039/C9RA07750B.

[71] T.T.T. Le, T.V. Vu, H. Kim, D.-S. Jeong, B. Pejjai, N.T.N. Truong, C. Park, Green and low-cost synthesis of CIGSe nanoparticles using ethanol as a solvent by a sonochemical method - A new approach, Mater. Chem. Phys. 207 (2018) 522–529, https://doi.org/10.1016/j.matchemphys.2017.12.078.

[72] S.M. McLeod, C.J. Hages, N.J. Carter, R. Agrawal, Synthesis and Characterization of 15% Efficient CIGSSe Solar Cells from Nanoparticle Inks, Prog. Photovolt.: Res. Appl. 23(11) (2015) 1550-1556. 10.1002/pip.2588.

[73] T.T.T. Le, N. Le, M.R. Pallavolu, Y. Jeon, D.-S. Jeong, B. Pejjai, V.R.M. Reddy, N. T.N. Truong, C. Park, Green and low-cost preparation of CIGSe thin film by a nanocrystals ink based spin-coating method, Korean J. Chem. Eng. 36 (12) (2019) 2110–2117, https://doi.org/10.1007/s11814-019-0386-8.

[74] L. Al Juhaiman, L. Scoles, D. Kingston, B. Patarachao, D. Wang, F. Bensebaa, Green synthesis of tunable Cu(In₁₋ₓGaₓ)Se₂ nanoparticles using non-organic solvents, Green Chem. 12(7) (2010) 1248-1252. 10.1039/C001813A.

[75] P.U. Londhe, A.B. Rohom, N.B. Chaure, Solar Cell Studies on CuIn₁₋ₓGaₓSe₂ Nanoparticles Derived from Chemical Reduction Process, Sol. Energy 206 (2020) 18–26, https://doi.org/10.1016/j.solener.2020.05.096.

[76] B.F. Gonçalves, P.M. Martins, A.P. LaGrow, G. Botelho, L.M. Salonen, S. Lanceros-Méndez, Y.V. Kolen'ko, Large-scale aqueous synthesis of Cu(In, Ga)Se₂ nanoparticles for photocatalytic degradation of ciprofloxacin, Dalton Trans. (2021), https://doi.org/10.1039/D1DT03557F.

[77] O. Stroyuk, A. Raevskaya, O. Selyshchev, V. Dzhagan, N. Gaponik, D.R.T. Zahn, A. Eychmüller, "Green" Aqueous Synthesis and Advanced Spectral Characterization of Size-Selected Cu₂ZnSnS₄ Nanocrystal Inks, Sci. Rep. 8 (1) (2018) 13677, https://doi.org/10.1038/s41598-018-32004-1.

[78] M.A. Abate, K. Dehvari, J.-Y. Chang, K. Waki, Aqueous synthesis of Mn-doped CuInSe₂ quantum dots to enhance the performance of quantum dot sensitized solar cells, Dalton Trans. 48 (42) (2019) 16115–16122, https://doi.org/10.1039/C9DT03163D.

[79] V.K. Kapur, A. Bansal, P. Le, O.I. Asensio, Non-vacuum processing of CuIn₁₋ₓGaₓSe₂ solar cells on rigid and flexible substrates using nanoparticle precursor inks, Thin Solid Films 431–432 (2003) 53–57, https://doi.org/10.1016/S0040-6090(03)00253-0.

[80] W. Wang, S.-Y. Han, S.-J. Sung, D.-H. Kim, C.-H. Chang, 8.01% CuInGaSe₂ solar cells fabricated from air-stable low-cost inks, Physical Chemistry Chemical Physics 14(31) (2012) 11154-11159. 10.1039/C2CP41969F.

[81] C.-H. Lu, J.-C. Sung, C.-Y. Ou, R.K. Singh, Solution-Processed Cu(In, Ga)(Se, S)₂ Solar Cells Prepared via a Surface Sulfurization Process, J. Taiwan Inst. Chem. Eng. 110 (2020) 41–50, https://doi.org/10.1016/j.jtice.2020.02.007.

[82] R. Chandran, S.K. Panda, A. Mallik, A short review on the advancements in electroplating of CuInGaSe₂ thin films, Mater. Renewable Sustainable Energy 7 (2) (2018) 6, https://doi.org/10.1007/s40243-018-0112-1.

[83] R. Kamada, T. Yagioka, S. Adachi, A. Handa, K. Tai, T. Kato, H. Sugimoto, New world record Cu(In, Ga)(Se, S)₂ thin film solar cell efficiency beyond 22%, in: 2016 IEEE 43rd Photovoltaic Specialists Conference (PVSC), 2016, pp. 1287–1291, https://doi.org/10.1109/PVSC.2016.7749822.

[84] D. Ohashi, T. Nakada, A. Kunioka, Improved CIGS thin-film solar cells by surface sulfurization using In₂S₃ and sulfur vapor, Sol. Energy Mater. Sol. Cells 67 (1) (2001) 261–265, https://doi.org/10.1016/S0927-0248(00)00290-7.

[85] B.J. Mueller, M. Mock, V. Haug, F. Hergert, T. Koehler, S. Zweigart, U. Herr, Ex-and in-situ investigations of sulfur diffusion into Cu(In, Ga)Se₂ thin films, Thin Solid Films 582 (2015) 284–289, https://doi.org/10.1016/j.tsf.2014.10.044.

[86] B.S. Yadav, S. Koppoju, S.R. Dey, S.R. Dhage, Microstructural investigation of inkjet printed Cu(In, Ga)Se₂ thin film solar cell with improved efficiency, J. Alloy. Compd. 827 (2020), 154295, https://doi.org/10.1016/j.jallcom.2020.154295.

[87] Y. Qu, G. Zoppi, N.S. Beattie, Selenization kinetics in Cu₂ZnSn(S, Se)₄ solar cells prepared from nanoparticle inks, Sol. Energy Mater. Sol. Cells 158 (2016) 130–137, https://doi.org/10.1016/j.solmat.2015.12.016.

[88] S.-C. Chen, N.-Z. She, K.-H. Wu, Y.-Z. Chen, W.-S. Lin, J.-X. Li, F.-I. Lai, J.-Y. Liang, C.W. Luo, L.-T. Cheng, T.-P. Hsieh, H.-C. Kuo, Y.-L. Chueh, Crystalline Engineering Toward Large-Scale High-Efficiency Printable Cu(In, Ga)Se₂ Thin Film Solar Cells on Flexible Substrate by Femtosecond Laser Annealing Process, ACS Appl. Mater. Interfaces 9 (16) (2017) 14006–14012, https://doi.org/10.1021/acsami.7b00082.

[89] T. Todorov, D.B. Mitzi, Direct Liquid Coating of Chalcopyrite Light-Absorbing Layers for Photovoltaic Devices, Eur. J. Inorg. Chem. 2010 (1) (2010) 17–28, https://doi.org/10.1002/ejic.200900837.

[90] C.J. Hibberd, E. Chassaing, W. Liu, D.B. Mitzi, D. Lincot, A.N. Tiwari, Non-vacuum methods for formation of Cu(In, Ga)(Se, S)₂ thin film photovoltaic absorbers, Prog. Photovoltaics Res. Appl. 18 (6) (2010) 434–452, https://doi.org/10.1002/pip.914.

[91] W. Septina, M. Kurihara, S. Ikeda, Y. Nakajima, T. Hirano, Y. Kawasaki, T. Harada, M. Matsumura, Cu(In,Ga)(S,Se)₂ Thin Film Solar Cell with 10.7% Conversion Efficiency Obtained by Selenization of the Na-Doped Spray-Pyrolyzed Sulfide Precursor Film, ACS Appl. Mater. Interfaces 7(12) (2015) 6472-6479. 10.1021/am507684x.

[92] X. Lin, R. Klenk, L. Wang, T. Köhler, J. Albert, S. Fiechter, A. Ennaoui, M.C. Lux-Steiner, 11.3% Efficiency Cu(In,Ga)(S,Se)₂ Thin Film Solar Cells via Drop-On-Demand Inkjet Printing, Energy Environ. Sci. 9(6) (2016) 2037-2043. 10.1039/C6EE00587J.

[93] F.C. Krebs, Fabrication and processing of polymer solar cells: A review of printing and coating techniques, Sol. Energy Mater. Sol. Cells 93 (4) (2009) 394–412, https://doi.org/10.1016/j.solmat.2008.10.004.

[94] H.-P. Kuo, H.-A. Tsai, A.-N. Huang, W.-C. Pan, CIGS absorber preparation by non-vacuum particle-based screen printing and RTA densification, Appl. Energy 164 (2016) 1003–1011, https://doi.org/10.1016/j.apenergy.2015.04.002.

[95] M.G. Faraj, K. Ibrahim, A. Salhin, Fabrication and characterization of thin-film Cu (In, Ga)Se₂ solar cells on a PET plastic substrate using screen printing, Mater. Sci. Semicond. Process. 15 (2) (2012) 165–173, https://doi.org/10.1016/j.mssp.2011.10.006.

[96] M.G. Faraj, K. Ibrahim, A. Salhin, Effects of Ga concentration on structural and electrical properties of screen printed-CIGS absorber layers on polyethylene terephthalate, Mater. Sci. Semicond. Process. 15 (2) (2012) 206–213, https://doi.org/10.1016/j.mssp.2012.03.002.

[97] A.C. Badgujar, R.O. Dusane, S.R. Dhage, Pulsed laser annealing of spray casted Cu (In, Ga)Se$_2$ nanocrystal thin films for solar cell application, Sol. Energy 199 (2020) 47–54, https://doi.org/10.1016/j.solener.2020.02.023.

[98] A.C. Badgujar, R.O. Dusane, S.R. Dhage, Cu(In, Ga)Se$_2$ thin film absorber layer by flash light post-treatment, Vacuum 153 (2018) 191–194, https://doi.org/10.1016/j.vacuum.2018.04.021.

[99] B.F. Gonçalves, G. Botelho, S. Lanceros-Méndez, Y.V. Kolen'ko, Eco-friendly and Cost-efficient Inks for Screen-printed Fabrication of Copper Indium Gallium Diselenide Photoabsorber Thin Films, J. Colloid Interface Sci. 598 (2021) 388–397, https://doi.org/10.1016/j.jcis.2021.04.059.

[100] Y.-F. Wang, T. Sekine, Y. Takeda, K. Yokosawa, H. Matsui, D. Kumaki, T. Shiba, T. Nishikawa, S. Tokito, Fully Printed PEDOT:PSS-based Temperature Sensor with High Humidity Stability for Wireless Healthcare Monitoring, Sci. Rep. 10 (1) (2020) 2467, https://doi.org/10.1038/s41598-020-59432-2.

[101] S.G.R. Bade, J. Li, X. Shan, Y. Ling, Y. Tian, T. Dilbeck, T. Besara, T. Geske, H. Gao, B. Ma, K. Hanson, T. Siegrist, C. Xu, Z. Yu, Fully Printed Halide Perovskite Light-Emitting Diodes with Silver Nanowire Electrodes, ACS Nano 10 (2) (2016) 1795–1801, https://doi.org/10.1021/acsnano.5b07506.

[102] T.M. Eggenhuisen, Y. Galagan, A.F.K.V. Biezemans, T.M.W.L. Slaats, W. P. Voorthuijzen, S. Kommeren, S. Shanmugam, J.P. Teunissen, A. Hadipour, W.J. H. Verhees, S.C. Veenstra, M.J.J. Coenen, J. Gilot, R. Andriessen, W.A. Groen, High efficiency, fully inkjet printed organic solar cells with freedom of design, J. Mater. Chem. A 3 (14) (2015) 7255–7262, https://doi.org/10.1039/C5TA00540J.

[103] A. Gheno, Y. Huang, J. Bouclé, B. Ratier, A. Rolland, J. Even, S. Vedraine, Toward Highly Efficient Inkjet-Printed Perovskite Solar Cells Fully Processed Under Ambient Conditions and at Low Temperature, Solar RRL 2 (11) (2018) 1800191, https://doi.org/10.1002/solr.201800191.

[104] D. Corzo, K. Almasabi, E. Bihar, S. Macphee, D. Rosas-Villalva, N. Gasparini, S. Inal, D. Baran, Digital Inkjet Printing of High-Efficiency Large-Area Nonfullerene Organic Solar Cells, Advanced Materials Technologies 4 (7) (2019) 1900040, https://doi.org/10.1002/admt.201900040.

[105] G. Tregnago, Printing organic photovoltaics, 537, Nat. Energy 3 (7) (2018), https://doi.org/10.1038/s41560-018-0212-2.

[106] A.H. Cheshme Khavar, A.R. Mahjoub, N. Taghavinia, Low-temperature solution-based processing to 7.24% efficient superstrate CuInS$_2$ solar cells, Solar Energy 157 (2017) 581–586, https://doi.org/10.1016/j.solener.2017.08.053.

[107] S. Nagino, H. Suzuki, S. Ueno, Substrate-Type Cu(In, Ga)Se$_2$ Solar Cells with All Layers Deposited by Non-Vacuum Solution-Based Methods, IEEE 39th Photovolt, Tampa, FL, USA, Spec. Conf., 2013, pp. 3475–3479.

[108] M. Singh, J. Jiu, T. Sugahara, K. Suganuma, Thin-Film Copper Indium Gallium Selenide Solar Cell Based on Low-Temperature All-Printing Process, ACS Appl. Mater. Interfaces 6 (18) (2014) 16297–16303, https://doi.org/10.1021/am504509r.

[109] A. Kovalenko, Hrabal, M., Printable Solar Cells, in: N.D. Sankir, Sankir, M. (Ed.), Printable Solar Cells2017, pp. 163-202. 10.1002/9781119283720.ch5.

[110] P. Jackson, R. Wuerz, D. Hariskos, E. Lotter, W. Witte, M. Powalla, Effects of heavy alkali elements in Cu(In,Ga)Se$_2$ solar cells with efficiencies up to 22.6%, Physica Status Solidi – Rapid Research Letters 10(8) (2016) 583-586. 10.1002/pssr.201600199.

[111] M. Wang, K.-L. Choy, All-Nonvacuum-Processed CIGS Solar Cells Using Scalable Ag NWs/AZO-Based Transparent Electrodes, ACS Appl. Mater. Interfaces 8 (26) (2016) 16640–16648, https://doi.org/10.1021/acsami.6b02137.

[112] M.A. Contreras, T. Barnes, J. van de Lagemaat, G. Rumbles, T.J. Coutts, C. Weeks, P. Glatkowski, I. Levitsky, J. Peltola, D.A. Britz, Replacement of Transparent Conductive Oxides by Single-Wall Carbon Nanotubes in Cu(In, Ga)Se$_2$-Based Solar Cells, J. Phys. Chem. C 111 (38) (2007) 14045–14048, https://doi.org/10.1021/jp075507b.

[113] M. Singh, P. Prasher, J. Kim, Solution processed silver-nanowire/zinc oxide based transparent conductive electrode for efficient photovoltaic performance, Nano-Structures & Nano-Objects 16 (2018) 151–155, https://doi.org/10.1016/j.nanoso.2018.05.009.

[114] D. Shin, T. Kim, B.T. Ahn, S.M. Han, Solution-Processed Ag Nanowires + PEDOT: PSS Hybrid Electrode for Cu(In, Ga)Se$_2$ Thin-Film Solar Cells, ACS Appl. Mater. Interfaces 7 (24) (2015) 13557–13563, https://doi.org/10.1021/acsami.5b02989.

[115] A. Kim, Y. Won, K. Woo, S. Jeong, J. Moon, All-Solution-Processed Indium-Free Transparent Composite Electrodes based on Ag Nanowire and Metal Oxide for Thin-Film Solar Cells, Adv. Funct. Mater. 24 (17) (2014) 2462–2471, https://doi.org/10.1002/adfm.201303518.

[116] Y.C. Xiao-Hui Tan, and Ye-Xiang Liu, Silver Nanowire Composite Thin Films as Transparent Electrodes for Cu(In,Ga)Se$_2$/ZnS Thin Film Solar Cells, Appl. Opt. 53 (15) (2014) 3273-3277. 10.1364/AO.53.003273.